Chapter 3

Radioactive Contamination and Vulnerability of Arctic Ecosystems

3.1. Introduction

Monitoring the levels and trends of man-made radionuclides in Arctic environments is a central part of the AMAP programme. The first AMAP assessment presented several radionuclide time series for the Arctic. Although, some of these have been extended in the present assessment, the main emphasis has been on the provision of new information. Milk is a key foodstuff which was not specifically addressed in the monitoring and trend section of the first assessment. To compensate for this, a number of time trends in ^{137}Cs and ^{90}Sr activity concentrations in milk are described below.

Although well known, the presence of ^{99}Tc and ^{129}I in the Arctic from fallout and earlier Sellafield discharges was not addressed in the first AMAP assessment because they were considered of less radiological significance than other radionuclides. However, increased rates of discharge from European reprocessing plants have raised awareness of these radionuclides, especially technetium, and brought the issue into political focus. Also, new information on remobilization of sedimented radionuclides from earlier discharges has made ^{239,240}Pu activity concentrations more relevant for current monitoring activities.

Available data have improved in terms of their quantity, the range of variables monitored, and the length of time series. This has enabled analysis of vulnerability for Arctic pathways of radiation with respect to three criteria: spatial variation in transfer rates, spatial variation in ecological half-lives, and variation in contamination between species. Radioecological vulnerability, which is also referred to as radioecological sensitivity (Howard, 2000), is considered in terms of the dose to man (or concentration in environmental compartment, if dose to man is not applicable) following a unit radionuclide input to the environment. The estimation of integrated transfer coefficients (Bq/m^3 per kBq/m^2) in the first AMAP assessment is an example of such analysis.

Five site-specific studies are included here, covering Arctic areas that were inadequately dealt with in the first assessment or for which significantly improved data are now available.

3.2. Atmosphere

Measurements of activity concentrations in the atmosphere provide one of the best means of detecting recent releases of radionuclides. Measurements in the surface atmosphere have not detected any significant new releases of artificial radioactivity over the last six years; in the Russian Arctic, for example, low mean annual concentrations in the surface atmospheric layer, of $<0.1\times10^{-5}$ Bq/m^3 of ^{137}Cs and $<0.02\times10^{-5}$ Bq/m^3 of ^{90}Sr, have been measured. Recently reported data for $^{239/240}$Pu deposition in Arctic Finland after the Chernobyl accident are also low at <0.25 Bq/m^2 (Paatero *et al.*, 2002).

The first AMAP assessment contained few air measurement data for Arctic areas in the early-1960s; the period of most intensive atmospheric nuclear weapons tests. Atmospheric ^{137}Cs activity concentrations in Finland are now available for a 40-year period (Figure 3·1). This dataset is based on measurements obtained at six sites and for different time periods. Because there is little spatial variation in precipitation across Finland, the data for the two southerly sites (Nurmijärvi and Seutula) from 1971 until the Chernobyl accident in 1986 are typical of Arctic conditions. The post-1995 data indicate

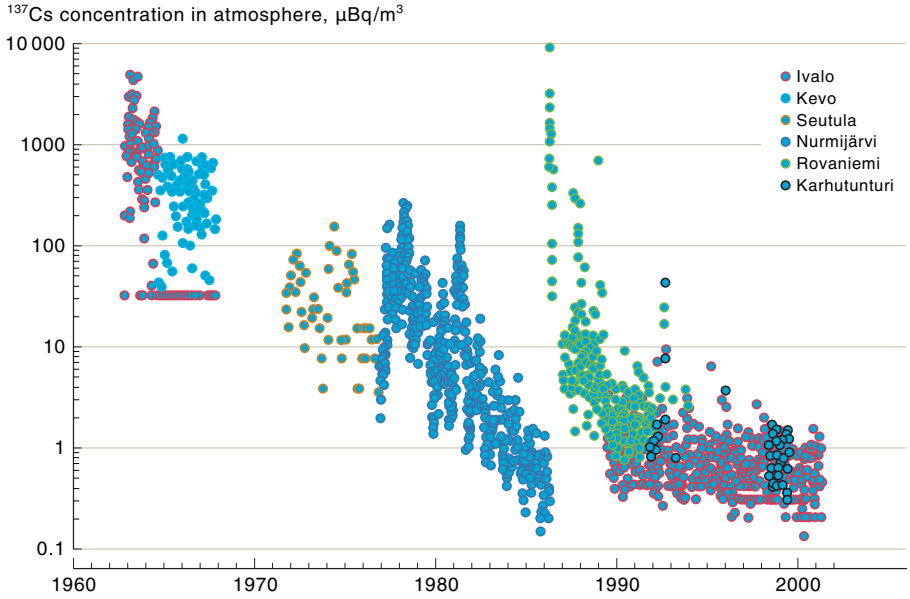

Figure 3·1. Atmospheric activity concentrations of ^{137}Cs at several sites in Finland.

lower levels in winter, due to snow cover, and higher levels when snow is not present, due to resuspension. The newly available data indicate higher values during the early-1960s than previously reported by AMAP for this period. Measurements at Ivalo during the peak period of global fallout are highly variable (Aaltonen *et al.*, 2002a).

Some new measurements from summer 1986 have also been made available since the first assessment (Aaltonen *et al.*, 2002b). After the Chernobyl accident, atmospheric ^{137}Cs activity concentrations in Arctic Finland were comparable to the peak values recorded in the 1960s, but the spatial variability was much greater.

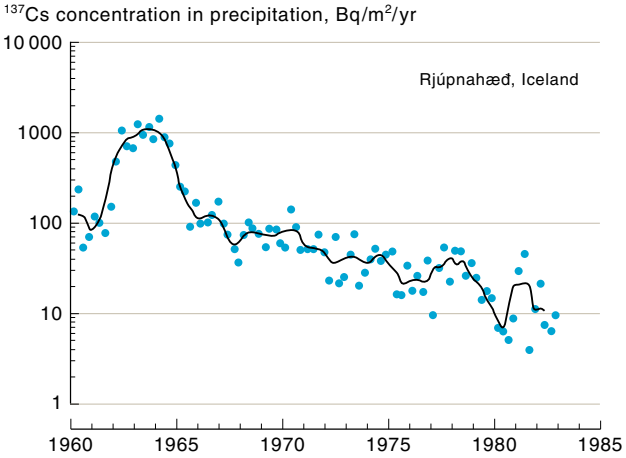

Figure 3·2. Activity concentrations of ^{137}Cs in precipitation at Rjúpnahæð (near Reykjavík). The points are quarterly measurements and the line a four-period moving average.

For Iceland, ^{137}Cs activity concentrations in precipitation at Rjúpnahæð (near Reykjavík) during the global fallout period are shown in Figure 3·2. Although the relevant time period is not shown on this graph, there was no detectable Chernobyl fallout in Iceland.

3.3. Marine environment

3.3.1. Technetium-99

Discharges from Sellafield in the 1970s and global fallout were mainly responsible for the initial occurrence of ^{99}Tc in Arctic seas. The recent increases in discharges from Sellafield are now the major source. Activity concentrations of around 20 to 25 Bq/kg dw were measured in the seaweed *Fucus vesicolosus* between 1994 and 1996 along the northern Norwegian coast (Yiou *et al.*, 2002). Using 1×10^5 as a concentration factor for the uptake, this corresponds to a seawater activity concentration of approximately 0.02 Bq/m^3.

A time series of ^{99}Tc activity concentrations in seawater at Hillesøy, a coastal location in northern Norway, showed an increase from 0.46 Bq/m^3 in summer 1997 to a maximum of 2.0 Bq/m^3 in early 2001. Following that peak, the levels steadily decreased to <1 Bq/m^3. For *Fucus vesiculosus*, activity concentrations increased from around 50 Bq/kg dw in July 1997 to >400 Bq/kg dw in January 2001. Concentrations then appeared to level off during 2001 and decrease throughout 2002, although more observations will be needed to confirm this trend (Figure 3·3). A comparison of ^{99}Tc activity concentrations in *Fucus* and seawater from this site indicates a concentration factor from water to *Fucus* in the

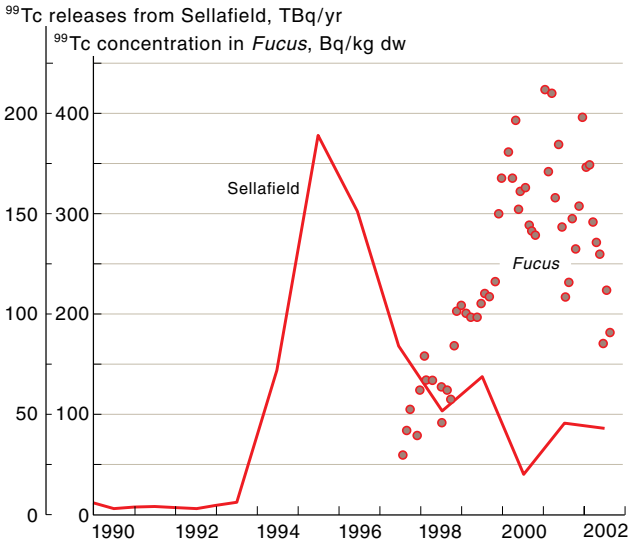

Figure 3·3. Temporal variation in ^{99}Tc activity concentrations in *Fucus* at Hillesøy (northern Norway) and releases from the Sellafield reprocessing plant (Kolstad and Lind, 2002).

range 1×10^5 to 2.6×10^5, as equilibrium between ^{99}Tc in the water and seaweed appears to occur slowly (Kolstad and Lind, 2002).

In 1999, ^{99}Tc activity concentrations observed along the Norwegian coast were associated with the peak releases from Sellafield in 1995, whereas those observed in Greenlandic and Icelandic waters were mainly due to releases from Sellafield and La Hague throughout the 1970s and 1980s. Global fallout levels are at least an order of magnitude lower than discharges from Sellafield (Dahlgaard, 1994; Dahlgaard *et al.*, 1995).

Karcher *et al.* (2003) simulated the ^{99}Tc distribution arising from Sellafield discharges between 1990 and 1999. This was done using a three-dimensional coupled ice-ocean model forced with daily variable atmospheric data (Karcher *et al.*, 2002). The ^{99}Tc was assumed to have been released from January 1990 onwards, with actual Sellafield discharge data input to the model at the North Channel in the northern Irish Sea. Figure 3·4 compares the model results for June 1999 with measured ^{99}Tc activity concentrations in the Northeast Atlantic in 1999. Predicted activity concentrations in the southern Barents Sea are in reasonable agreement with measured values. Values measured around Greenland, Iceland, and the Faroe Islands are mainly influenced by pre-1990 discharges and are not represented by the model.

3.3.2. Iodine-129

Levels of the naturally occurring long-lived iodine isotope ^{129}I have been elevated substantially over the past decades, initially due to atmospheric nuclear weapons tests and subsequently due to emissions from nuclear fuel reprocessing (see Figure 2·3). Atmospheric weapons tests resulted in an increase in the ratio between radioactive ^{129}I and its stable counterpart, ^{127}I, in the surficial compartments (i.e., surface soils, surface seawater, and freshwaters) of the Northern Hemisphere from 10^{-12} to 10^{-10}.

The iodine isotope ratio (and other radionuclide ratios such as ^{129}I:^{137}Cs and ^{129}I:^{99}Tc) can be used to trace the movement of water masses from the Norwegian Coastal Current into the Arctic basin and the At-

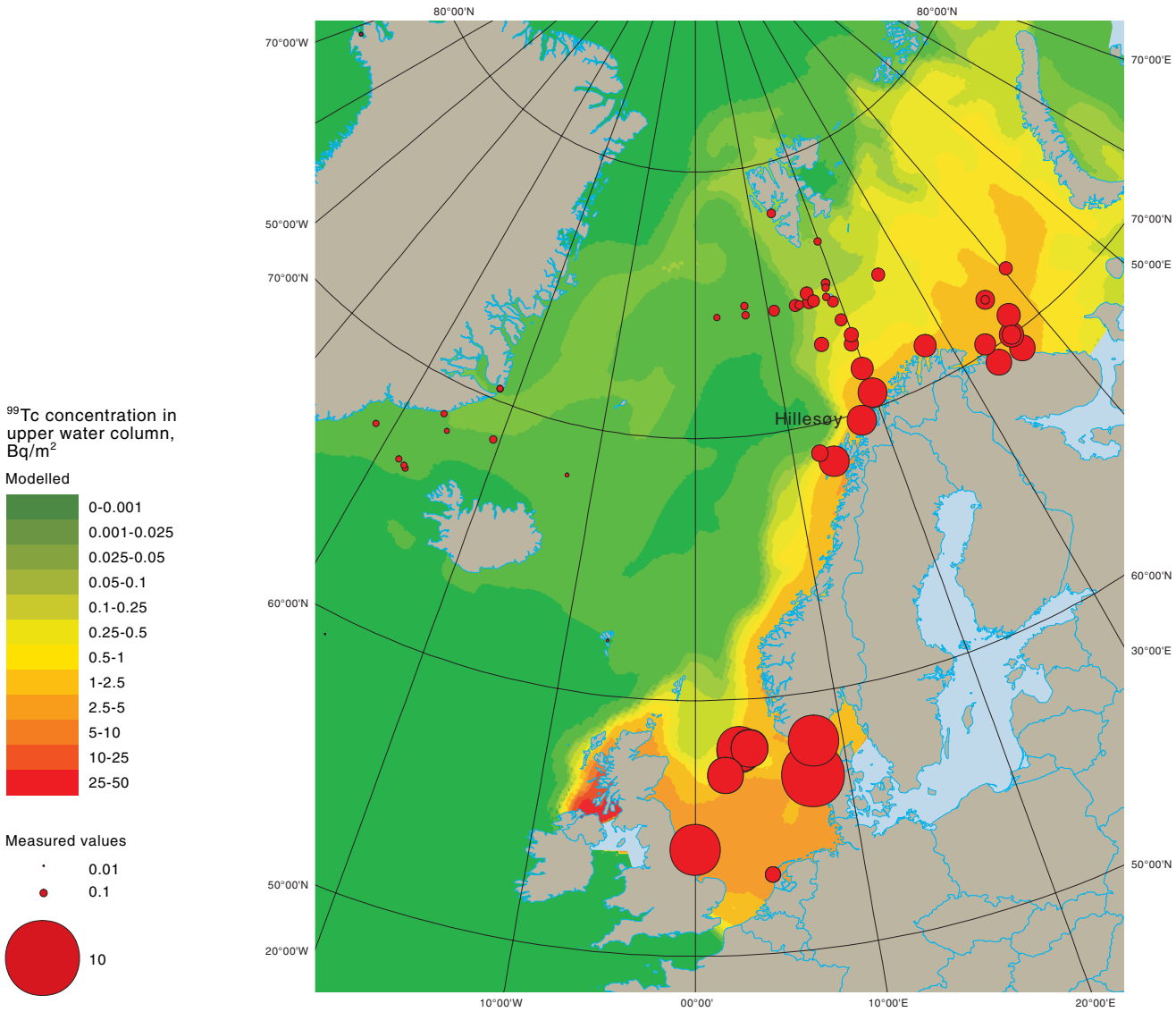

Figure 3·4. Simulated distribution of ^{99}Tc concentrations in the upper 20 m of the water column in June 1999 (Karcher *et al.*, 2003). Concentration is represented by the color coding. The red circles show measured values in 1999.

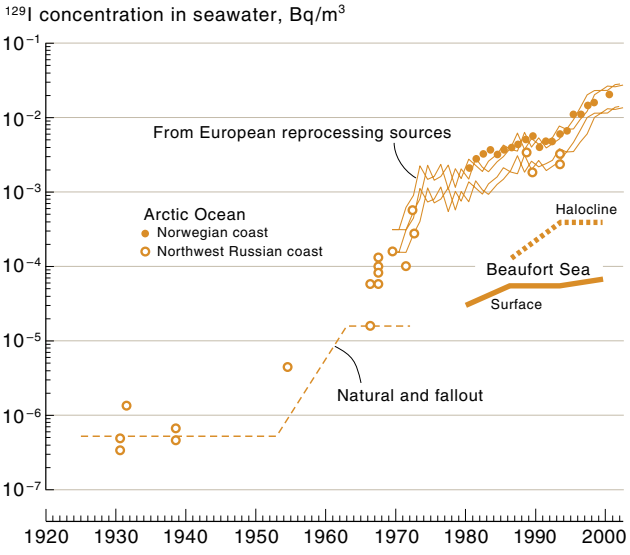

Figure 3·5. Activity concentrations of ^{129}I in the Arctic Ocean near the entry of Atlantic Water (Norway and northwestern Russia) and the Beaufort Sea (Cooper *et al.*, 1998, 1999; Matishov *et al.*, 2002; Raisbeck and Yiou, 1999; Smith *et al.*, 1998, 1999; Yiou *et al.*, 2002).

lantic Deep Water. Along the northern Norwegian and northwest Russian coasts, ^{129}I levels, and hence the isotope ratio, have been orders of magnitude higher than the global fallout level since the late-1970s. Measurements taken one month after the *Kursk* submarine accident in August 2000 did not indicate any leakage of ^{129}I from the *Kursk*, but confirmed the high levels and increasing trend of ^{129}I activity concentrations in Atlantic water entering the Arctic Ocean (Figure 3·5). The activity concentration of ^{129}I from European reprocessing sources in water entering the Arctic Ocean may be predicted using dilution factors of 1 to 2×10^{-14} yr/m^3 and transit times of 2 to 3 yr (Cap de la Hague) and 4 to 5 yr (Sellafield) (Figure 3·5). This is in agreement with earlier studies on other radionuclides (e.g., AMAP, 1998; Dahlgaard, 1994). In the Beaufort Sea, levels in the halocline water masses have increased as a result of ^{129}I transported from the Atlantic Ocean through the Arctic Ocean; whereas in surface waters it is mainly fallout-derived ^{129}I of Pacific origin that has been detected. The transport time for the Atlantic halocline waters across the Arctic Basin is in the order of one to two decades (AMAP, 1998; Smith *et al.*, 1998, 1999).

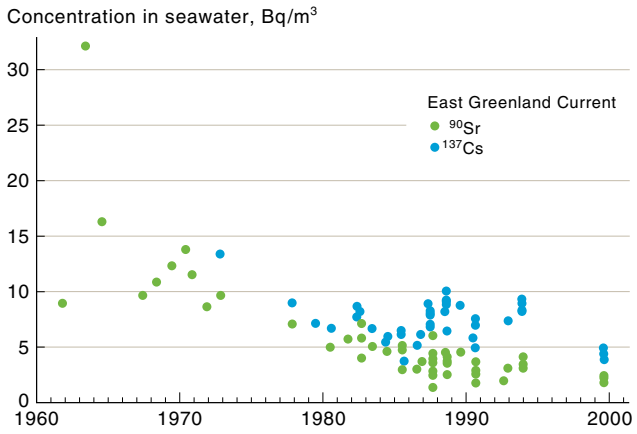

Figure 3·6. Time trends for ^{137}Cs and ^{90}Sr in the East Greenland Current (between 10.7°E and 22.35°E, and 70°N and 81.9°N).

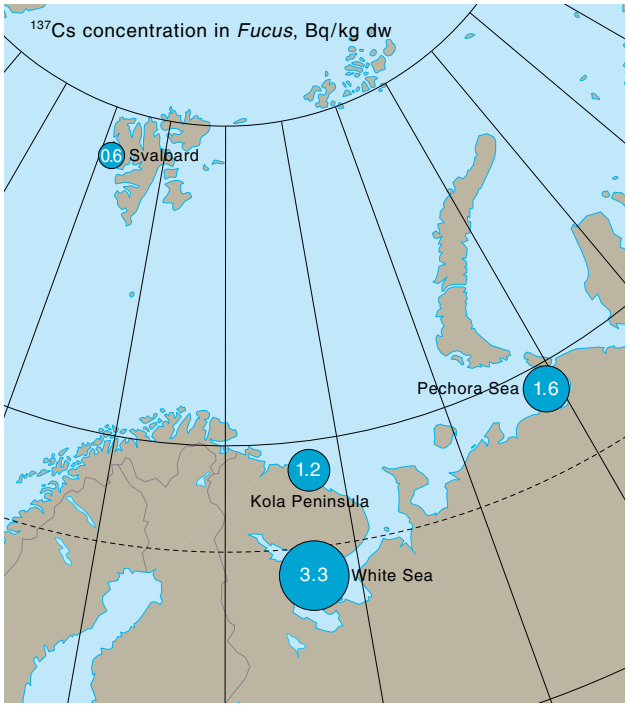

Figure 3·7. Activity concentrations of ^{137}Cs in *Fucus* (Rissanen *et al.*, 1995).

3.3.3. Cesium-137 and ^{90}Sr

Changes with time in ^{137}Cs and ^{90}Sr activity concentrations in surface seawater in the East Greenland Current (where the highest levels generally occur around Greenland) are shown in Figure 3·6. Whereas ^{90}Sr activity concentrations in seawater decrease with an effective ecological half-life (T_{eff}; Box 3·1) of approximately nine years, those of ^{137}Cs level off and even increase during the late-1980s and early-1990s due to fallout from the Chernobyl accident and inputs from European reprocessing plants.

Recent measurements of ^{137}Cs activity concentrations in *Fucus* spp. in the Barents, Pechora, and White Seas are shown in Figure 3·7. The highest values were detected in the White Sea.

Recent data (1993 to 1998) on the spatial distribution of ^{137}Cs in sediments from Arctic areas indicate considerable variability (Figure 3·8). Activity concentrations in areas with no known local sources of anthropogenic radionuclides are <20 Bq/kg dw. Higher levels occur in the White Sea and off the Norwegian coast (up to 60 Bq/kg dw) in areas strongly affected by Chernobyl fallout, in the outer parts of the Yenisey estuary (up to 80 Bq/kg dw), near the Atomflot base in the Kola fjord (up to 200 Bq/kg dw) and in the dumping areas along the western coast of Novaya Zemlya (up to 10^5 Bq/kg dw).

Consistently low ^{137}Cs activity concentrations have been reported in a range of marine fish species (Table 3·1). Except for dab (*Limanda limanda*) and capelin (*Mallotus villosus*), no significant differences were found between the various species. Dab (with low levels) were

Table 3·1. Activity concentrations for ^{137}Cs in marine fish species (Bq/kg ww) for 1995 to 2000 (AMAP Data Centre).

	n	Mean ± SD
Haddock (*Melanogrammus aeglefinus*)	65	0.25 ± 0.11
Cod (*Gadus* spp.)	394	0.22 ± 0.08
Shorthorn sculpin (*Myoxocephalus scorpius*)	10	0.31 ± 0.16
Flounder (*Platichthys flesus*)	6	0.33 ± 0.06
Capelin (*Mallotus villosus*)	3	0.16 ± 0.08
Dab (*Limanda limanda*)	247	0.09 ± 0.03

Box 3·1. *Effective ecological half-lives*

The effective ecological half-life (T_{eff}) describes the time required for the activity concentration of a radionuclide in an environmental compartment (often a food product) to be reduced to one half of its original activity concentration. It therefore incorporates physical decay. The ecological half-life (T_{ec}) does not take physical decay into account, and thus can be adapted for different isotopes of the same element. For example, the T_{eff} of ^{134}Cs and ^{137}Cs will differ because of the differences in physical half-lives, while the T_{ec} would be identical. The relationship between T_{eff} and T_{ec} for a radionuclide with a physical half-life (T_{phys}) will be:

$$T_{eff} = (T_{phys} \cdot 1/T_{ec})/(T_{phys} + 1/T_{ec})$$

Where data on long time trends are available, it is possible to model changes with time in activity concentrations. As a given radionuclide often exists in the environment in different physical/chemical forms, with different mobilities, a multiple exponential function is needed to describe the changes. In practice, a double exponential is often used, of the form:

$$A(t) = A_0 \cdot \left(a \cdot \exp\left(-\frac{\ln 2}{T_1} \cdot t\right) + (1-a) \cdot \exp\left(-\frac{\ln 2}{T_2} \cdot t\right)\right) \qquad \text{Eqn. 3.1}$$

where $A(t)$ is the activity concentration at time t, A_0 is the initial activity, T_1 and T_2 are the effective ecological half-lives (T_{eff1} and T_{eff2}) or the ecological half-lives (T_{ec1} and T_{ec2}); and a is a parameter partitioning the decay between the two half-lives. In this case, the shorter half-life will dominate the decay for the first period, and the longer half-life will govern the process on a longer time scale.

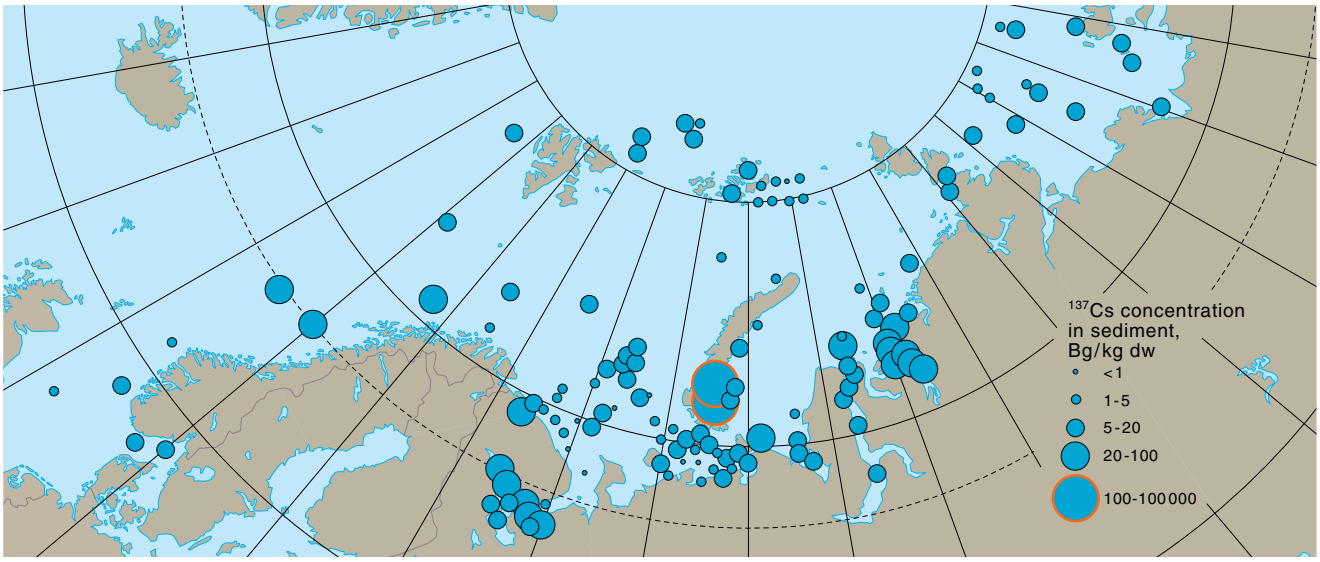

Figure 3·8. Distribution of ^{137}Cs in surface sediments from 1993 to 1998.

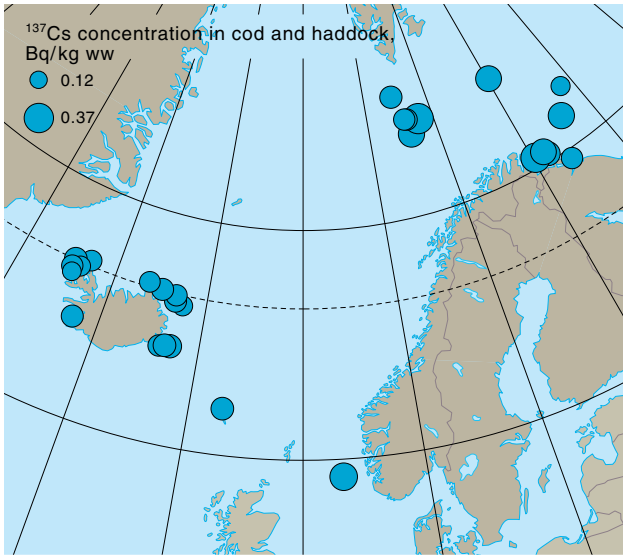

Figure 3·9. Average ^{137}Cs activity concentrations in cod and haddock from 1995 to 2000.

sampled near Iceland, where ^{137}Cs levels in seawater are generally low. Figure 3·9 shows the spatial variation in mean ^{137}Cs activity concentrations in cod (*Gadus* spp.) and haddock (*Melanogrammus aeglefinus*) from 1995 to 2000.

3.3.4. Plutonium isotopes

The ^{239,240}Pu activity concentration in surface waters of northern seas ranged from 2 to 66 mBq/m^3 in 1995 (Figure 3·10). The highest ^{239,240}Pu activity concentrations occurred in surface seawater off the north and northeast coasts of Scotland. This is consistent with findings on remobilized plutonium (Pu) from Irish Sea sediments as a newly identified source of Pu, with a typical ^{238}Pu : ^{239,240}Pu isotope ratio of around 0.2 (see Section 2.2.3).

The ^{238}Pu : ^{239,240}Pu isotope ratios in waters, particularly in the Norwegian Sea and Barents Sea, are elevated above the expected fallout ratio of ~0.04 and are, in some cases, close to Irish Sea ratios. The isotope ratios therefore suggest that Sellafield-derived Pu may have

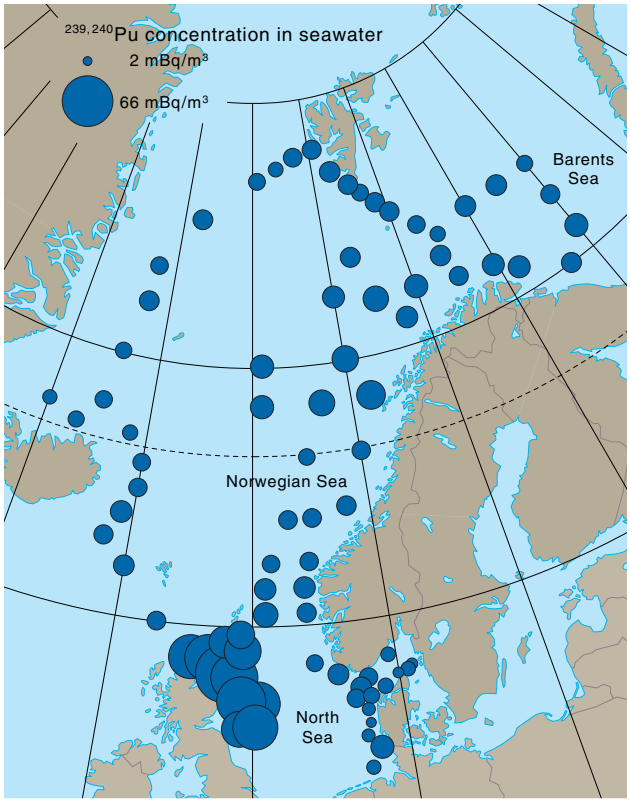

Figure 3·10. Distribution of ^{239,240}Pu in surface seawater of the northern seas in 1995 (Grøttheim, 2000).

been transported with the currents into the Norwegian Sea and the Barents Sea and, to a lesser extent, even the Greenland Sea. The ratios indicate that Sellafield could have been a major contributor to the Pu concentrations observed in Scottish and Norwegian waters (Grøttheim, 2000; Herrmann *et al.*, 1998; Kershaw *et al.*, 1999), whereas the primary source in the Arctic Ocean and the Greenland Sea remains global fallout. However, in two surveys of Pu in seawater in various parts of the Arctic Ocean, Vintró *et al.* (2002) explained the observed concentrations by advection of global fallout Pu from mid-North-Atlantic latitudes to the Arctic Ocean and failed to see evidence of Sellafield Pu.

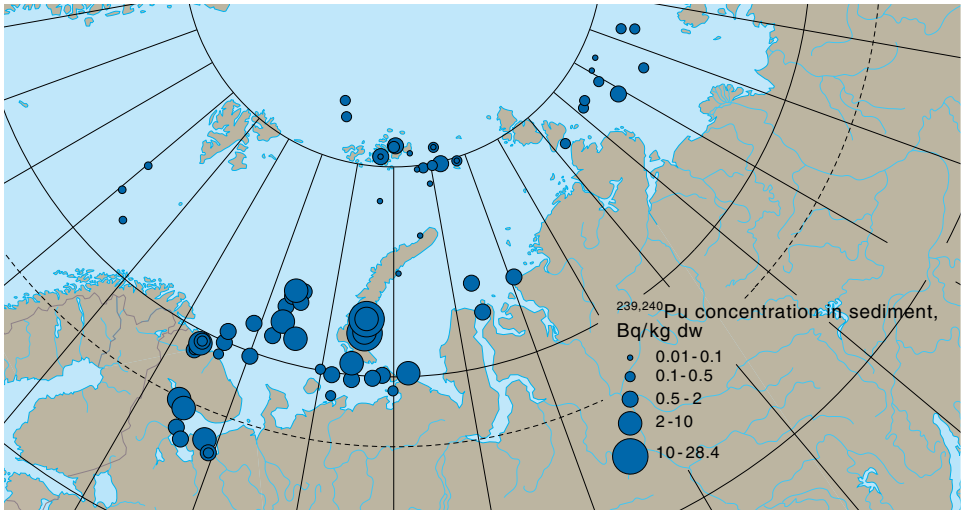

Figure 3·11. Activity concentrations of ^{239,240}Pu in surface sediments 1996 to 2000.

Figure 3·11 shows Pu activity concentrations in surface sediments. Global fallout levels in marine sediments depend on many factors such as sediment characteristics, depth, and proximity to river outflows. As is the case for seawater, isotope ratios may indicate different origins, but the actual global fallout concentrations in surface sediments vary considerably. Cooper *et al.* (2000) found Pu isotope ratios in Arctic Ocean sediments to be due to global fallout in most cases, and failed to show any indications of a Sellafield contribution, in accordance with the results for seawater (Vintró *et al.*, 2002).

Rissanen *et al.* (2000) analyzed 92 fish samples from commercial operations in the Barents Sea and found ^{239,240}Pu in one sample only: a ray, *Raja radiata*, containing 7.9 and 4.9 mBq/kg ww in flesh and bones, respectively. Plutonium activity concentrations were below detection limits of 1 to 3 mBq/kg ww in all other samples.

3.3.5. Radionuclide behavior in marine systems

3.3.5.1. Partitioning and uptake

Water movement and sedimentation are of major importance in determining transport pathways and the fate of radioactive material released to, or transported within, the marine environment. One of the important geochemical factors affecting the transport of radionuclides is particle-water exchange. In water, radionuclides are partitioned between the dissolved and particulate phases. Partitioning depends on the chemical form of the radionuclide, the physical–chemical properties of the chemical analogues (usually elemental analogues), and the characteristics of the environment.

Biological uptake and associated dose assessments for human exposure generally depend on the levels of dissolved radionuclides in water, although filter feeders (mussels and oyster) accumulate radionuclides from the particulate phase. For biota that are closely associated with marine sediments, such as benthic infauna and epifauna, sediment concentrations can exert the primary influence on the extent of uptake.

3.3.5.2. Transport of radionuclides in sea ice

Sea ice transport is a unique pathway in polar areas (Pfirman *et al.*, 1995, 1997; Strand *et al.*, 1996) that is partially independent of water mass movement (Pfirman *et al.*, 1997). During sea ice formation, dissolved contaminants are rejected together with salt. Levels of dissolved contaminants are therefore lower in sea ice than in seawater (Weeks, 1994). Consequently, the main focus in ice transport studies has been on the transport and fate of radionuclides associated with sediment particles incorporated into the ice, derived both from particles suspended in seawater and from bottom sediments.

A radiological assessment of sea ice transport has been considered by Iosjpe and Borghuis (2000) and Iosjpe (2002). Their approach is based on box modelling (Iosjpe *et al.*, 1997, 2002) that incorporates the various transfers of radioactivity: from the liquid phase to ice; from suspended sediment and bottom sediment to ice; through sea ice transport between sea areas; and into seawater during ice melt.

The potential significance of sea ice transport in the dispersion of radionuclides within the marine environment was illustrated by modelling the transport of radionuclides from the Kara Sea to the Fram Strait through the Arctic Ocean following the simulated release of 1 TBq of specific radionuclides into Ob Bay in the Kara Sea. Dispersion through the Kara Sea to the Fram Strait is particularly interesting because the model indicated that sea ice transport of contaminants in this region may represent a more rapid transport pathway than water. Furthermore, modelling showed the effect to be directly proportional to the partition coefficient (Kd) of each radionuclide. Thus, sea ice transport seems more relevant for high-Kd elements such as ^{241}Am and ^{60}Co and less important for ^{137}Cs and ^{90}Sr which are principally associated with the dissolved phase (Iosjpe and Strand, 2002).

3.3.6. Vulnerability in marine pathways

Marine ecosystems are relatively less vulnerable to atmospheric inputs of radiocesium than freshwater and terrestrial environments. This is due to the capacity of most marine ecosystems to rapidly dilute an input of radioactive contaminants through processes such as advection and mixing, coupled with the large volumes of water generally involved, and the high ionic strength of the saline waters. Thus, short-term consequences are likely to be more important in marine ecosystems as dilution is a long-term process. Vulnerable marine ecosys-

tems include those into which liquid discharges are released – especially if their exchange with the World Ocean is slow or restricted, as is the case for some fjords and inlets. In an Arctic context, this could include areas that receive radionuclides transported from nuclear facilities by marine currents or rivers such as the Ob and Yenisey. In addition to man-made radionuclides, marine areas may receive natural radioactivity from non-nuclear industries.

Radioecological vulnerability in marine ecosystems is affected by a number of factors, such as water exchange rates; residence times for radionuclides in the water column; sediment and sedimentation properties, including bioturbation and resuspension; freshwater inflow; salinity; oxygenation of the water column and sediments; and ice conditions.

Marine zones with high biological productivity are considered radioecologically vulnerable, when considering collective doses. From an economic point of view, highly productive areas such as the Barents Sea and areas used for aquaculture of mollusks, fish, or crustaceans are potentially important.

3.4. Freshwater environment

Estimates of the initial activity concentration in water bodies following radionuclide deposition can be made by assuming dilution of activity 'deposited' to the river or lake surface. Therefore, deep rivers and lakes would be expected, initially, to be less vulnerable than shallow water bodies. However, deposition times can be long, as was the case for global fallout, compared to river water transit times. Catchment runoff can also make a significant long-term contribution to water activity concentrations. Activity concentrations in runoff water decline significantly with time after deposition. At a given point in time, the activity concentration in river or lake water per unit of deposition to the catchment (the *runoff coefficient*) is a measure of radioecological vulnerability of the catchment. Organic, boggy catchments, such as those prevailing in some Arctic areas, have much higher ^{137}Cs runoff coefficients than catchments with a high proportion of mineral soils (Kudelsky *et al.*, 1996).

Loss of the initial input of radioactivity from lake and reservoir water may be estimated using the water residence time of the lake and simple models for the removal of radioactivity to sediments. Long-term activity concentrations in lakes with relatively short water residence times are primarily controlled by inputs of radioactivity from the surrounding catchment. Long-term activity concentrations in closed lakes, which have relatively long water residence times, are controlled by the transfer of radioactivity to and from bottom sediments. Lakes with high vulnerability for radiocesium include shallow lakes with long water residence times, especially those having large catchments with a high percentage of organic boggy soils, as these allow higher runoff than catchments with other soil types. In areas such as Finnish Lapland, vulnerability to radiocesium is high due to the presence of boggy soils (30 to 60% of catchments) combined with a hilly topography that may increase surface runoff.

When contaminated snow melts, radionuclides may be transported with runoff waters and may then contaminate soils and freshwater systems. Contamination from snow melt can be highly heterogeneous and radionuclide contents in soil can be higher in areas where water from melting snow accumulates. The effect varies with the size of the catchments and lakes. Ice overlying lakes can, to some extent, protect freshwater biota from radioactive contamination. However, when the ice melts there is a sudden influx of contamination, in addition to that from melting snow. Thus, there can be a delayed pulse of enhanced activity concentrations in spring.

Currently, atmospheric and surface terrestrial activity concentrations of ^{129}I in the Northern Hemisphere exceed those due to global fallout by up to six orders of magnitude near point sources (Sellafield, Cap de la Hague, Chernobyl), three to four orders of magnitude in most of Western Europe, and at least an order of magnitude outside Europe (e.g., Moran *et al.*, 1999). In the Arctic, little is known about terrestrial ^{129}I levels, but some indications based on analyses of freshwaters and precipitation suggest an increase of about two orders of magnitude above the nuclear weapons test (NWT) contaminated background levels (Moran *et al.*, 1999), and four orders of magnitude above the natural background level in most of the Arctic. For freshwaters, where current ^{129}I:^{127}I ratios are typically up to an order of magnitude lower than in terrestrial food chains within the same region, very few data are available for rivers and estuaries without evident contamination (Beasley *et al.*, 1997; Fehn and Snyder, 2000; Meili *et al.*, 2002). Levels are far higher in some Russian rivers into which discharges from point sources, such as the Mayak reprocessing plant, occur, reaching about three and four orders of magnitude above the NWT background level near the mouths of the Yenisey and Ob rivers, respectively (Cochran *et al.*, 2000; Cooper *et al.*, 1998).

3.4.1. Rivers

The first AMAP assessment reported temporal changes in ^{137}Cs and ^{90}Sr activity concentrations in Finnish and Russian rivers. Figure 3·12 shows the extended time series for ^{90}Sr activity concentrations in the water of different Russian rivers. Current levels are low in all areas of the Russian Arctic.

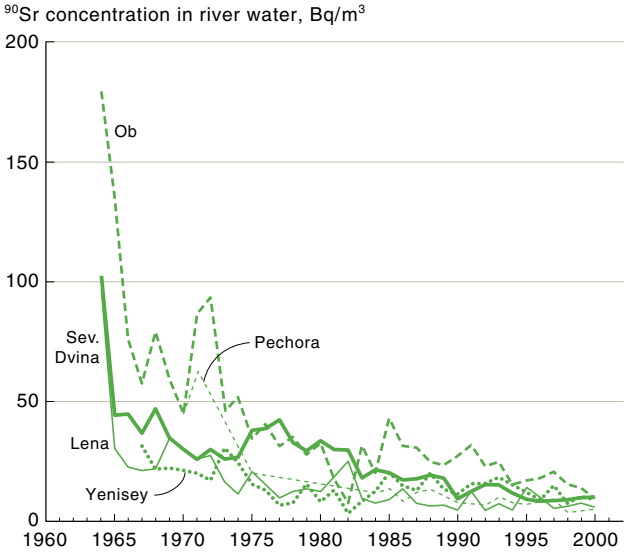

Figure 3·12. Changes in ^{90}Sr activity concentrations in Russian rivers since the mid-1960s.

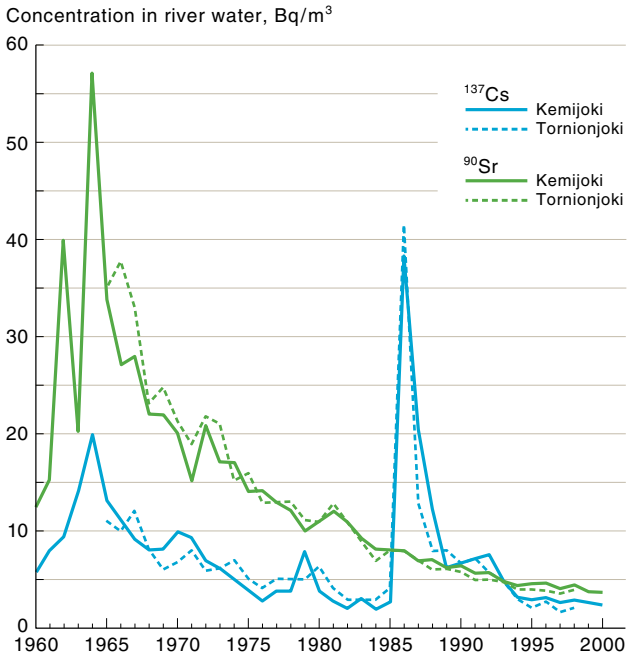

Figure 3·13. Annual mean levels of ^{137}Cs and ^{90}Sr in two Finnish rivers since 1960.

Updated information for two Finnish Arctic rivers (Figure 3·13) shows further declines over the last five years, following the Chernobyl accident (1986). In the global weapons testing period, ^{90}Sr activity concentrations in rivers were consistently two- to three-fold higher than for ^{137}Cs. Chernobyl deposition reversed this situation such that activity concentrations of ^{137}Cs were higher than ^{90}Sr for some years following deposition. However, owing to the shorter effective half-life (T_{eff}; Box 3·1) of ^{137}Cs compared with ^{90}Sr, activity concentrations of ^{90}Sr have been slightly higher than for ^{137}Cs since 1994.

Table 3·2 compares T_{eff} values for ^{90}Sr in various Russian rivers.

Table 3·2. T_{eff} values for ^{90}Sr in Russian rivers.

	T_{eff_1} (yr)	T_{eff_2} (yr)
Severnaya Dvina	12.9±1.7*	
Ob	0.7±0.3	13.2±2.4
Lena	0.2±0.15	14.3±2.2

Half-lives calculated using non-linear least squares (www.r-project.org).

* It was not possible to calculate a double exponential for Severnaya Dvina.

Data for ^{90}Sr and ^{137}Cs in two Finnish rivers (Saxen, 2003) show that post-Chernobyl T_{eff} values for ^{137}Cs are about a factor of two shorter than the bomb-fallout half-lives (Table 3·3). As different periods of time were used to calculate the half-lives in Tables 3·2 and 3·3, the first components of the T_{eff} for the Finnish and Russian rivers are not comparable, but the second components are not significantly different.

3.4.2. Fish

Long-term data for Russia which enable a comparison of ^{137}Cs activity concentrations in freshwater fish from two Arctic regions indicate that concentrations in fish from the Kola Peninsula are statistically significantly

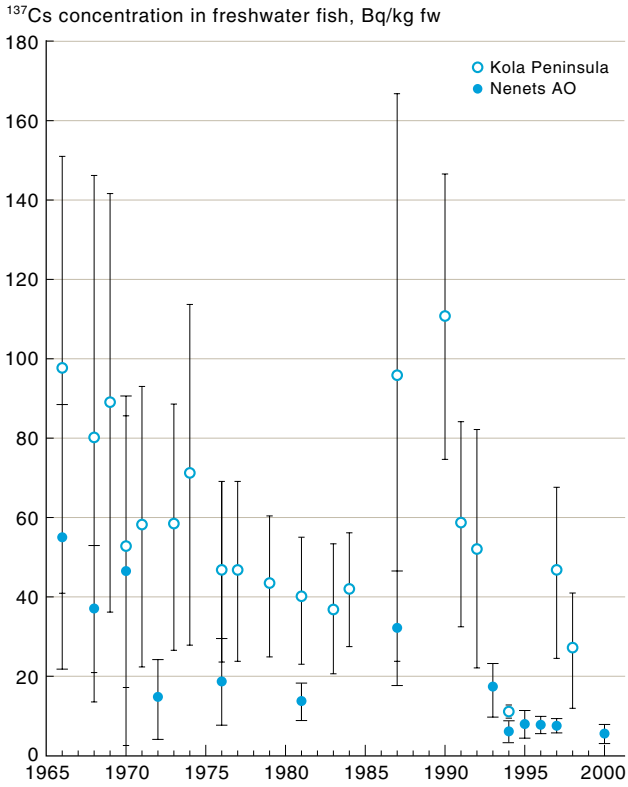

Figure 3·14. Activity concentrations (±SD) for ^{137}Cs in freshwater fish from the Kola Peninsula and Nenets AO.

higher than in fish from lakes and rivers in the Nenets Autonomous Okrug (NAO), both after the period of global fallout and after the deposition of Chernobyl fallout (Figure 3·14). A contributory factor was the higher Chernobyl fallout on the Kola Peninsula than in the NAO.

Table 3·3. T_{eff} values (yr) for ^{90}Sr and ^{137}Cs in Finnish rivers from weapons test and Chernobyl fallout (based on Saxen, 2003).

		Weapons tests	Chernobyl	
		1965-1985	1988-2000	1965-2000
^{90}Sr	Tornionjoki	9.1	11.6	9.5
	Kemijoki	10.5	12.8	11.6
		1965-1985	1986-1988	1989-2001
^{137}Cs	Tornionjoki	9.3	0.6	4.2
	Kemijoki	10.4	1.0	5.1

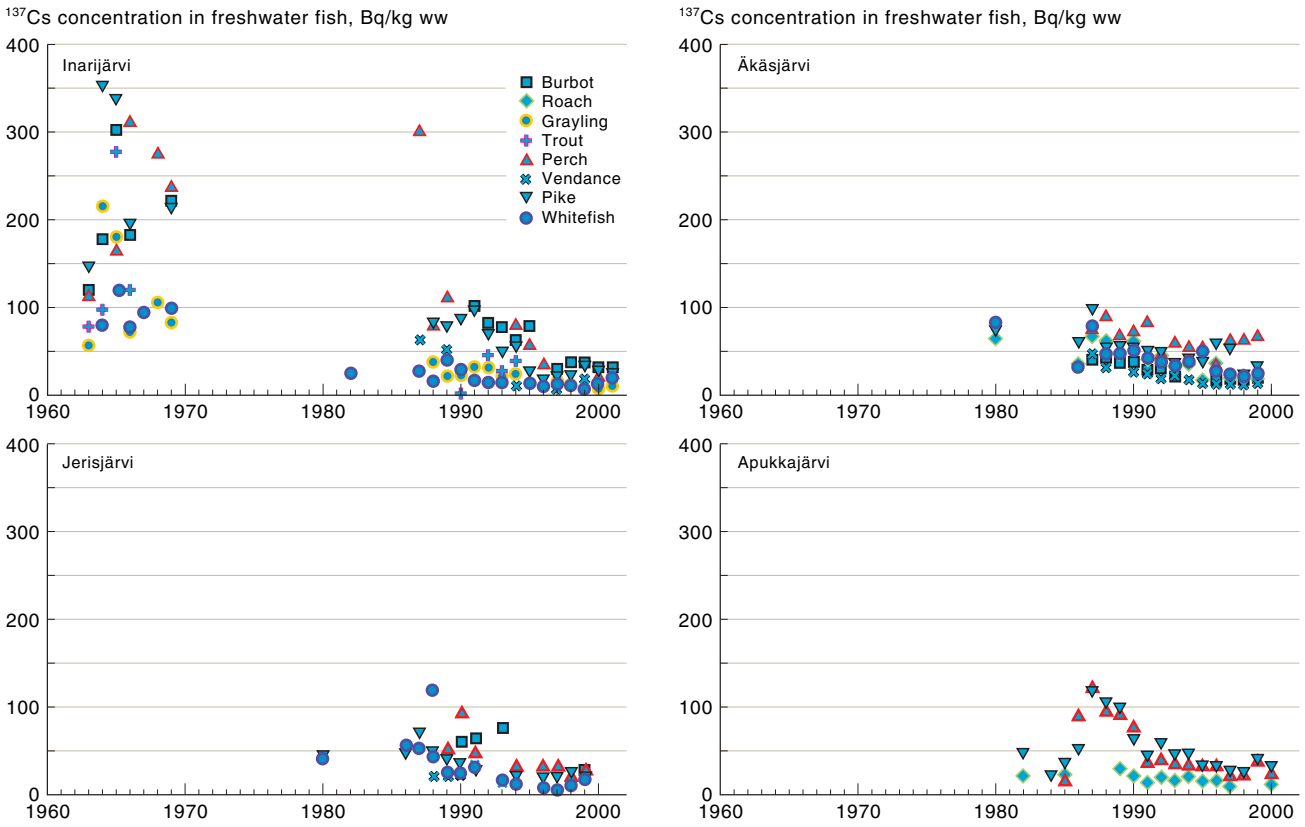

Figure 3·15. Changes in ^{137}Cs activity concentrations with time in various fish species in four lakes in Arctic Finland.

Also, fish from the Kola Peninsula are mainly caught in lakes (particularly, Lake Lovozero), whereas they are mainly from rivers in the NAO, and fish caught in lakes are generally more contaminated than fish from rivers.

3.4.2.1. Species differences

Activity concentrations are available for ^{137}Cs in a large number of different fish species for four Finnish lakes: Inarijärvi, a large lake in northeast Finland (Pasvik area, Barents Sea catchment); Apukkajärvi, a small highly eutrophic lake in the vicinity of Rovaniemi (Kemijoki catchment area); and Äkäsjärvi and Jerisjärvi, which are two medium-sized lakes in the Tornionjoki system 200 km northwest of Rovaniemi (Figure 3·15). In Inarijärvi, the only lake sampled in Arctic Finland during the global fallout period, ^{137}Cs activity concentrations of up to 356 Bq/kg ww were measured in pike in 1964 (Kolehmainen *et al.*, 1966). In 1982, activity concentrations of 25 Bq/kg ww occurred in whitefish from Inarijärvi (STUK, 1983). After the Chernobyl accident, when more data became available, there was a single high measurement of 305 Bq/kg ww in perch, but otherwise ^{137}Cs activity concentrations were much lower than in the 1960s with maximum values of ~100 Bq/kg ww.

Radiocesium activity concentrations in fish are inversely related to the potassium (K) concentration of the surrounding water (e.g., Blaylock, 1982; Kolehmainen *et al.*, 1967). Similarly, an inverse relationship has been found between ^{90}Sr activity concentrations in fish and water calcium (Ca) concentrations (e.g., Blaylock, 1982). High K or Ca concentrations in water are often a result of the runoff of agricultural fertilizers, but this is not particularly relevant to Arctic ecosystems. Transfer rates to fish also depend on feeding habit, with ^{137}Cs activity concentrations in the more radioecologically-vulnerable predatory fish generally a factor of two or more higher than for non-predatory fish. The Finnish Arctic data are diverse and thus difficult to analyze, however, it is clear that some species generally contain lower radionuclide activity concentrations than others. For each lake sampled, ^{137}Cs activity concentrations are higher in pike (a predatory species) and perch (partially predatory) than in other species, and whitefish contamination is consistently low.

3.4.2.2. Migratory fish

Salmon (*Salmo salar*) from Arctic seas migrate up the Tana River, which flows from northern Finland, through Norway to the Barents Sea, to spawn. They are an important traditional food resource for the indigenous peoples living near the river and the present total catch varies from 90 to 180 t/yr. Annual samples show the activity concentrations of ^{137}Cs in flesh to have decreased from 1 Bq/kg ww in 1988 to 0.3 Bq/kg ww in 2000, with T_{eff} values of 6 yr over the study period. In comparison, Baltic salmon from the more heavily Chernobyl-contaminated Bothnian Bay had activity concentrations 100 times higher (Rissanen and Ikäheimonen, 2000).

3.5. Terrestrial environment

3.5.1. Soil and humus

Recent data demonstrate that ^{137}Cs deposition from 1995 to 2002 at the Zapolyarie and North monitoring stations, covering the Asian and European parts of the Russian Arctic respectively, has not exceeded 1.3 Bq/m^2/yr.

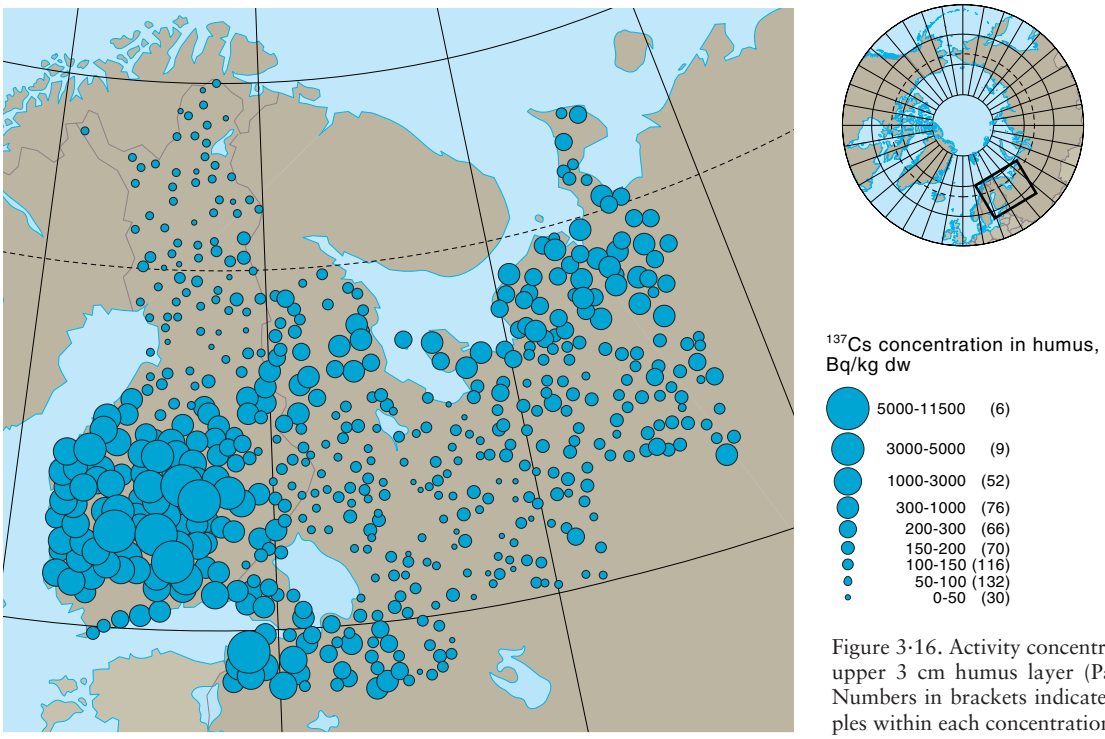

Figure 3·16. Activity concentrations of ^{137}Cs in the upper 3 cm humus layer (Paatero *et al.*, 2002). Numbers in brackets indicate the number of samples within each concentration range.

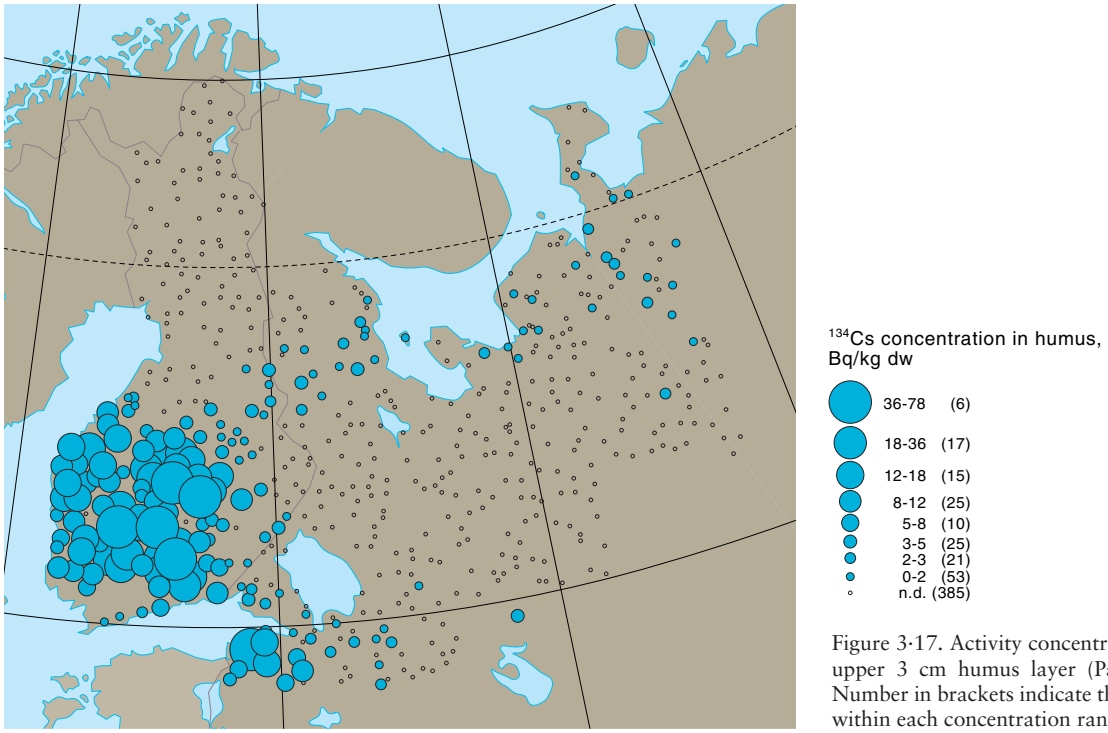

Figure 3·17. Activity concentrations of ^{134}Cs in the upper 3 cm humus layer (Paatero *et al.*, 2002). Number in brackets indicate the number of samples within each concentration range.

A comprehensive survey of ^{137}Cs and ^{134}Cs in the upper 3 cm humus layer in Finland and northwest Russia in 2000 (Figures 3·16 and 3·17) found ^{134}Cs (from the first plume) from the Chernobyl accident could still be detected in southern Finland and near St Petersburg. The presence of ^{134}Cs suggests that the elevated ^{137}Cs levels in this area are also due to the Chernobyl accident. Paatero *et al.* (2002) found a similar pattern to that of the humus survey for Chernobyl-derived Pu fallout in Finland.

Activity concentrations of 9 to 32 Bq/m^2 were found for ^{239,240}Pu in surface vegetation and in the upper 3 to 5 cm of soils near the coast in northwest Russia and Svalbard between 1993 and 1996. The variation was due to the type and density of the surface vegetation (Rissanen *et al.*, 2001). The ^{238}Pu : ^{239,240}Pu ratio at these sites and in Franz Josef Land suggests the primary source is global fallout.

The time of deposition is critical for Arctic ecosystems, particularly for short-term deposition, such as might occur after an accident. In subarctic areas, snow cover is present for about seven to eight months of the year, the period during which the land is snow-covered increasing with increasing latitude and factors such as

altitude, and distance from coasts. When deposition occurs onto snow, the radioactivity is available for uptake by vegetation and biota only after the snow has melted. Surface contamination of plants, lichens, and mosses occurs as snow melts, by a process similar to interception of wet deposition. The extent of foliar uptake depends on the rapidity of snow melt, the topography of the landscape and the morphology of the vegetation. Subsequent lateral transport of radionuclides from melting snow depends on the extent of interception and catchment characteristics at both the large and small scale. If deposition occurs in the few months when vegetation is exposed to the atmosphere, then the transfer of radioactivity to herbivores is more rapid. Furthermore, for short-lived radionuclides, especially ^{131}I, deposition only leads to contamination of foodstuffs if it occurs just prior to, or during, the growing season.

The uptake of radioactivity by plants from soil occurs via the soil solution. The processes controlling radionuclide transfer between soil components and the soil solution are critical for bioavailability. For example, sorption of many radionuclides on non-specific cationic exchangeable sites is weaker than on more specific sites such as clay minerals. In addition, soil solution composition is important because of the competition between radionuclides and their stable analogues, e.g., strontium and Ca, and cesium and K. Therefore, soils with low potassium and clay mineral content will be more radioecologically vulnerable to radiocesium than soils with high potassium and clay mineral content. Strong sorption enhances retention of radionuclides in upper soil layers where most roots absorb nutrients. It is not clear whether the presence of a thin, organic layer in many Arctic ecosystems will enhance or reduce radionuclide mobility, nor is the effect of permafrost known.

3.5.2. Mushrooms

After the Chernobyl accident, the potential importance of mushroom consumption as a source of radiocesium intake became apparent, especially in the mid- to long-term after the accident. The first AMAP assessment found the importance of mushroom consumption to vary considerably between countries and population groups. Although a potentially important source, data on ^{137}Cs contamination of mushrooms at Arctic sites were not generally available. Such data are now available for Finland, Russia, and Norway.

3.5.2.1. Finland

Figure 3·18 shows the results of an extensive survey in Arctic Finland of fruiting bodies from a wide range of mushroom species (Rissanen *et al.*, 2002) The samples were obtained from 1983 onwards from four forest types at a site 70 km southeast of Rovaniemi. In 1993, the average ^{137}Cs deposition to the soil at the site was 0.8 to 0.9 kBq/m^2 declining to 0.7 to 0.8 kBq/m^2 in 1999. Owing to the low level of Chernobyl fallout in Finnish Lapland, about half the total ^{137}Cs present was due to global fallout.

There was no significant difference in the ^{137}Cs activity concentration of the mushroom species between the four types of forest stand. Analysis of the ^{134}Cs content showed that significant pre-Chernobyl ^{137}Cs was present in many species, again with about half the total ^{137}Cs

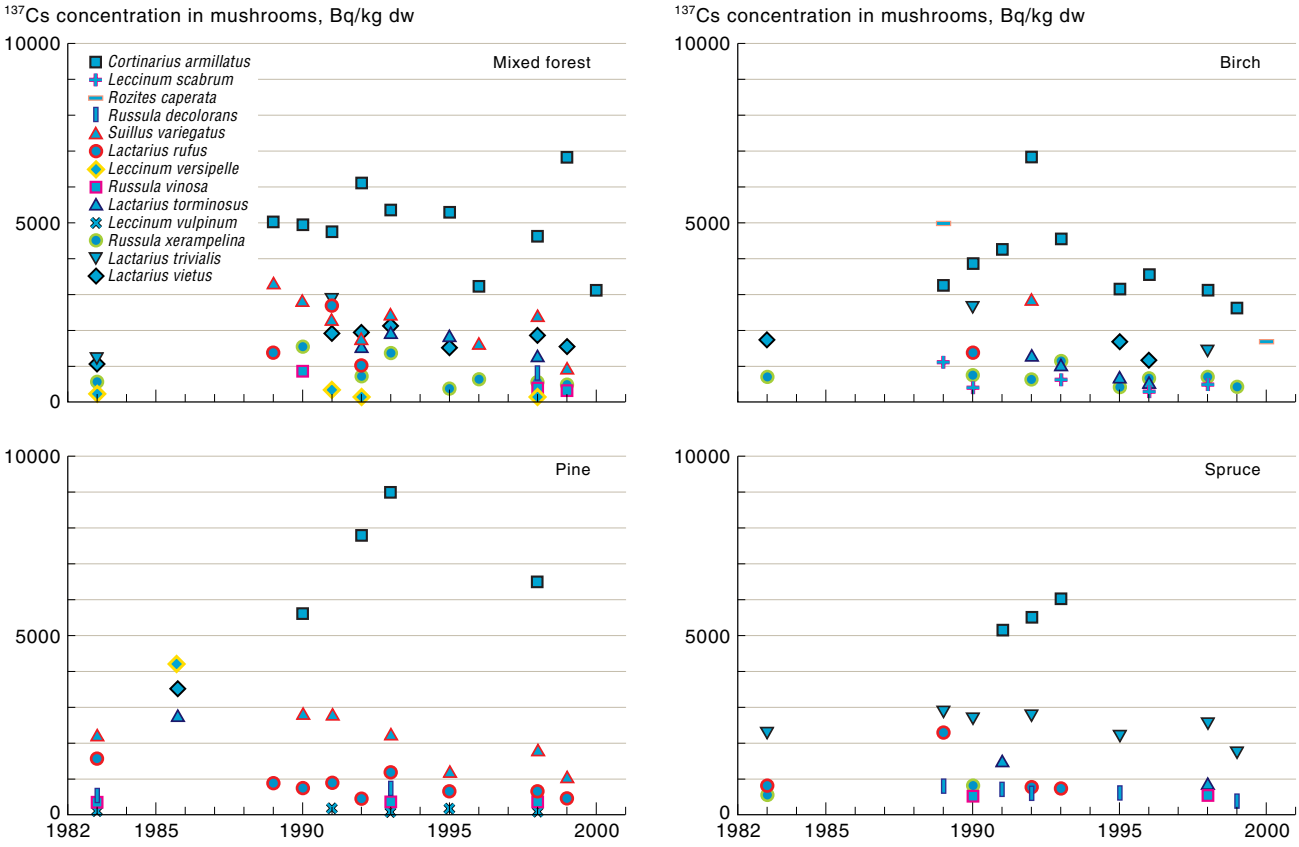

Figure 3·18. Activity concentrations of ^{137}Cs in a range of mushroom species in Finnish forest stands.

Box 3·2. *Aggregated transfer coefficients*

The transfer of radionuclides is quantified using the aggregated transfer coefficient (T_{ag}) defined as the activity concentration in an environmental compartment (often a food product) (in Bq/kg) divided by the corresponding radionuclide deposition in soil (in Bq/m^2); with units of m^2/kg.

$$T_{ag} = \frac{Activity\ concentration}{Deposition}$$

T_{ag} values were most commonly used in the former Soviet Union to quantify transfer to food products. In other countries, they are most often used for semi-natural products. They are therefore the most commonly used transfer quotient for Arctic ecosystems. High T_{ag} values, such as those derived for highly organic soils for radiocesium, indicate radioecologically vulnerable areas. T_{ag} values are time dependent, and can be combined with ecological half-lives to quantify changes with time. They are not appropriate for use when considering surface depositions onto plants during fallout.

The T_{ag} may be combined with the effective ecological half-life as follows:

$$C(t) = A \cdot T_{ag_0} \cdot \exp(-\lambda_r \cdot t) \cdot \left(a_1 \cdot \exp\left(-\frac{\ln 2}{T_{eff1}} \cdot t\right) + (1 - a_1) \cdot \exp\left(-\frac{\ln 2}{T_{eff2}} \cdot t\right)\right) \quad \text{Eqn. 3.2}$$

where $C(t)$ is the activity concentration of a given radionuclide in a food product at time t (Bq/kg); A is the surface deposition of radionuclide p (Bq/m^2); T_{ag_0} is the initial value of the aggregated transfer coefficient (m^2/kg); λ_r is the radioactive decay constant for radionuclide p (1/days); t is the time after deposition (days); and the other parameters are the same as in Equation 3.1 (Box 3·1).

The values of parameters T_{ag_0}, a_1, T_{eff1}, and T_{eff2} can be estimated on the basis of long-term measurements of ^{137}Cs and ^{90}Sr activity concentrations in different food products during the period of global fallout (about 40 years) and after the Chernobyl accident.

Using these techniques, it is possible to calculate integrated transfer coefficients (ITC) for ^{137}Cs and ^{90}Sr in different regions (AMAP, 1998). The calculation, assuming a single deposition event uses the formula:

$$ITC = \int_0^\infty \frac{C(t)dt}{A} = T_{ag_0} \cdot \int_0^\infty \exp(-\lambda_r \cdot t) \cdot \left(a_1 \cdot \exp\left(-\frac{\ln 2}{T_{eff1}} \cdot t\right) + (1 - a_1) \cdot \exp\left(-\frac{\ln 2}{T_{eff2}} \cdot t\right)\right) dt \quad \text{Eqn. 3.3}$$

or, after integration:

$$ITC = T_{ag_0} \cdot \left(a_1 \cdot \frac{T_{eff1}}{\ln 2} + (1 - a_1) \cdot \frac{T_{eff2}}{\ln 2}\right), \quad \text{(Bq/yr)/kg per kBq/m}^2 \quad \text{Eqn. 3.4}$$

In the case of ^{137}Cs, some areas received an additional input from the Chernobyl accident. As this input was a pulse input and possibly in a different chemical form, separate half-lives must be calculated for the Chernobyl input after removing the contribution from global fallout by extrapolating the pre-Chernobyl data using the model.

from Chernobyl and half from global fallout. The highest pre-Chernobyl value was 2390 Bq/kg dw in *Lactarius trivialis* in 1983. Although the variable nature of the data makes derivation of half-lives difficult, it is clear that ^{137}Cs uptake persists for many years in a wide variety of mushroom species.

After the Chernobyl accident, the most highly contaminated species in all four forests was the non-edible *Cortinarius armillatus*, with a maximum recorded value of 9030 Bq/kg dw in 1993. Of the edible species, the most contaminated were *Rozites caperata*, *Lactarius trivialis*, and *Suillus variegatus*, which is consistent with data for mushrooms in temperate areas.

3.5.2.2. **Russia**

Activity concentrations of ^{137}Cs in mushroom fruiting bodies from northwest Russia in 1989 to 1999 were low compared to those recorded in temperate areas of Europe. Highest activity concentrations were recorded in *Lactarius flexuosus* and *Xerocomus* spp. Over the period 1987 to 2000, ^{137}Cs T_{ag} values (Box 3·2) from soil to mushroom for two regions in northwest Russia were relatively constant (RTCP, 1999, 2000; Shutov *et al.*, 1999). Therefore, in Table 3·4, data from the whole sampling period have been collated to quantify transfer for the Kola Peninsula and the Mezen and NAO regions.

Table 3·4. Activity concentrations for ^{137}Cs in mushroom species (Bq/kg, mean ± SD, air dw) in northwest Russia for 1992 to 2000 and associated T_{ag} values (m^2/kg ± SD) for soil to mushroom (Borghuis *et al.*, 2002).

	Kola Peninsula			Mezen and Nenets AO regions		
	n	Activity concentration	T_{ag}	n	Activity concentration	T_{ag}
Leccinium aurantiacum	126	27.6±1.7	0.013±0.0007	27	21.8±3.9	0.0072±0.0012
Leccinium scabrum	63	55.2±5.3	0.026±0.0025	28	27.8±5.4	0.0082±0.0017
Suillus bovines	–	–	–	2	35.0±7.1	0.0104±0.0031
Russula spp.	70	63.9±4.5	0.029±0.002	19	54.4±11.3	0.016 ±0.0032
Paxillus spp.	–	–	–	5	45.3±20.3	0.016 ±0.0073
Xerocomus spp.	36	117 ±9	0.053±0.0044	4	77.4±20.9	0.028 ±0.0075
Lactarius rufus	6	133 ±21	0.067±0.01	5	59.4±8.5	0.018 ±0.0025
Lactarius flexuosus	3	235 ±69	0.144±0.042	4	98.3±36.8	0.035 ±0.013
Lactarius necator	14	50.3±9.5	0.026±0.0048	2	40.3±3.7	0.014 ±0.0013
Boletus edulis	1	8.9	0.0047	5	22.4±5.3	0.0075±0.0017
Suillus luteus	11	80 ±14	0.037±0.0066	1	40	0.013

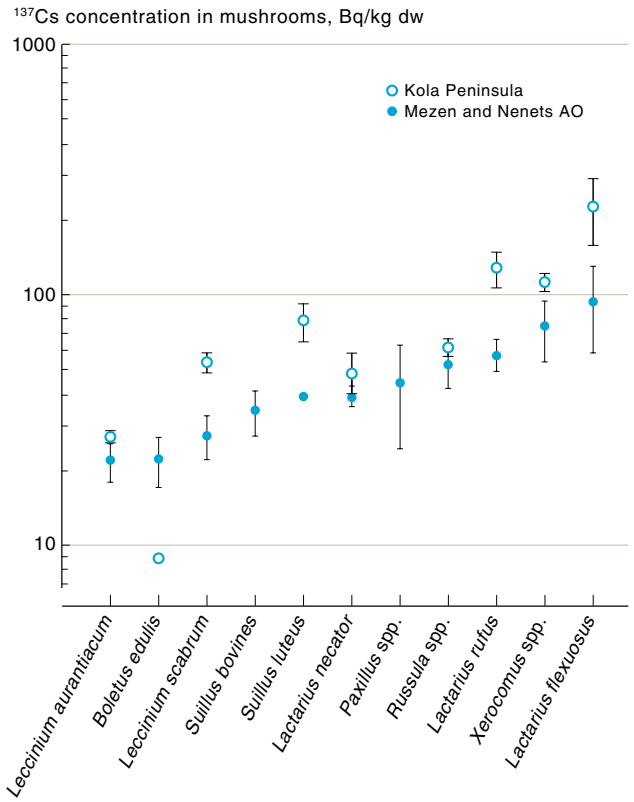

Figure 3·19. Activity concentrations of ^{137}Cs in various mushroom species from the Kola Peninsula and the Mezen and Nenets AO regions (Borghuis *et al.*, 2002).

The average ^{137}Cs T_{ag} values from soil to mushroom on the Kola Peninsula were significantly higher than for the NAO region (P = 0.00024, Table 3·4 and Figure 3·19).

3.5.2.3. Norway

Activity concentrations of ^{137}Cs in mushroom species from Troms and Finnmark collected in 1998 to 1999 are given in Table 3·5. Activity concentrations vary significantly between species. The activity concentration in species such as *Rozites caperata*, which is known to accumulate cesium, was a factor of ten to fifteen higher than in *Leccinum* spp. The activity concentration of ^{137}Cs in fungi with a high cesium transfer was about 500 times higher than in plant species from the same site, whereas the factor was approximately 50 for fungi with a moderate transfer.

Table 3·5. Activity concentrations for ^{137}Cs in mushroom species (Bq/kg dw ± SD) in Arctic Norway for 1998 to 1999 and corresponding T_{ag} values (m^2/kg ± SD) for soil to mushroom (Salbu, pers. comm., 2001).

	n	Activity concentration	T_{ag}
Boletus edulis	1	2097	2.17
Leccinum spp.	2	354 ± 175	0.37 ± 0.14
Rhozites caperata	4	3929 ± 3557	4.38 ± 4.47
Russula spp.	5	595 ± 417	0.48 ± 0.43

The T_{ag} values also varied between the different species. Species with a known high uptake of ^{137}Cs had a ten-fold higher T_{ag} value for ^{137}Cs than those with a lower uptake.

Overall, the data indicate lower activity concentrations in Arctic mushroom species than in those from nearby temperate areas of NW Europe due to the low levels of global and Chernobyl fallout in most of the areas sampled. Nevertheless, the ^{137}Cs activity concentrations are higher in mushrooms than in many other Arctic foodstuffs. There is, however, evidence of large T_{ag} values. Although activity concentrations in the most contaminated species vary between areas, the data are not directly comparable as different weight bases have been used.

3.5.3. Berries

Activity concentrations of ^{137}Cs in the berries of cloudberry (*Rubus chamaemorus*), bilberry (*Vaccinium myrtillus*), and cowberry (*Vaccinium vitis-idaea*) were measured at four sites in Lapland. In 1980 to 1981, before the Chernobyl accident, ^{137}Cs activity concentrations at Kittilä were 25 to 45 Bq/kg ww in cloudberry, 11 to 19 Bq/kg ww in bilberry, and 6 to 22 Bq/kg ww in cowberry (Rissanen *et al.*, 1987). Sufficient data were available at one of the four sites, Salla-Kuusamo, to indicate a slow change in concentration since the Chernobyl accident (Figure 3·20) and higher ^{137}Cs activity concentrations in cloudberry berries than in those of bilberry or cowberry.

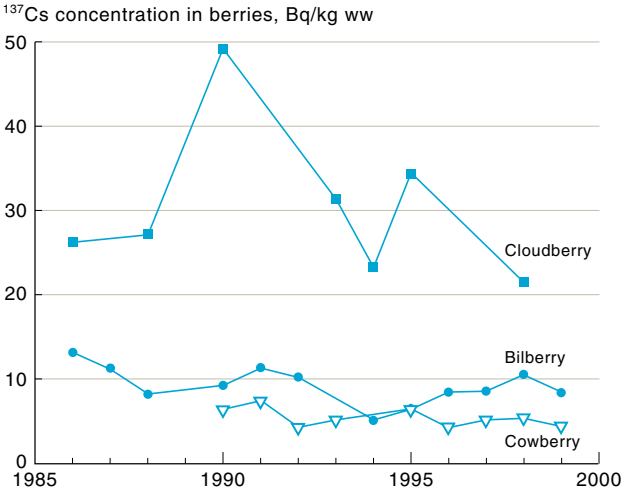

Figure 3·20. Changes over time in ^{137}Cs activity concentrations in three species of berries at Salla-Kuusamo in Lapland, Finland (Rissanen *et al.*, 1987).

The range in activity concentrations in these species at the four sites in Lapland since the Chernobyl accident is shown in Table 3·6. Despite the difficulties in comparing data with some time dependency after the Chernobyl accident, the sampling frequencies for the four species are sufficiently similar to conclude that there are differences between the species and that cloudberry is the most contaminated.

Table 3·6. Range in ^{137}Cs activity concentrations (Bq/kg ww) for berry species in Lapland for 1986 to 2001 (Rissanen, pers. comm., 2002).

	Rovaniemi	Inari	Salla-Kuusamo	Kittilä
Cloudberry	30-63	16-31	21-49	30-38
Bilberry	6-15	2-9	5-13	10-16
Cowberry	4-25	2-7	4-8	2-12

Table 3·7. Average ^{137}Cs activity concentrations for various berry species (Bq/kg ww; mean ± SE) in northwest Russia for 1998 to 1999 and associated T_{ag} values (m^2/kg) for soil to berries (Borghuis *et al.*, 2002).

	Kola Peninsula			Mezen and Nenets AO regions		
	n	Activity concentration	T_{ag}	n	Activity concentration	T_{ag}
Cloudberry	28	31.6±1.4	0.014±0.0007	50	26.9±2.3	0.0091±0.0008
Bilberry	64	11.1±1.0	0.0048±0.0004	24	14.2±1.3	0.0045±0.0004
Cowberry	192	7.2±0.4	0.0032±0.0002	40	3.7±0.4	0.0013±0.0002
Cranberry	5	17.9±4.7	0.0091±0.0024	38	11.6±1.1	0.0037±0.0004

Activity concentrations and T_{ag} values for ^{137}Cs in various berry species collected in 1998 to 1999 in northwest Russia are shown in Table 3·7. Activity concentrations and transfer of ^{137}Cs to cloudberry are higher than for the other species, including bilberry which is often the most contaminated berry in temperate areas.

Recent data on ^{137}Cs activity concentrations in the berries of bilberry and cloudberry from Arctic Norway in 1998 to 1999 are shown in Table 3·8 (note the data are on a dry and not wet weight basis). Although, there was a tendency for higher ^{137}Cs activity concentrations in cloudberry than bilberry the difference was not statistically significant. Some samples also contained ^{134}Cs from the Chernobyl accident (with maximum values of 33 Bq/kg dw in cloudberry and 45 Bq/kg dw in bilberry).

Table 3·8. Activity concentrations for ^{137}Cs (Bq/kg dw (Bq/kg ww*)) in bilberry and cloudberry in Arctic Norway for 1998 to 1999 (Salbu, pers. comm., 2001).

	n	Mean	Minimum	Maximum
Cloudberry	11	74.8 (11.2)	32.0 (4.8)	175.0 (26.5)
Bilberry	15	63.1 (9.5)	nd	167.0 (25.1)

nd: not detectable;
* fresh weight values estimated assuming 85% water content in berries.

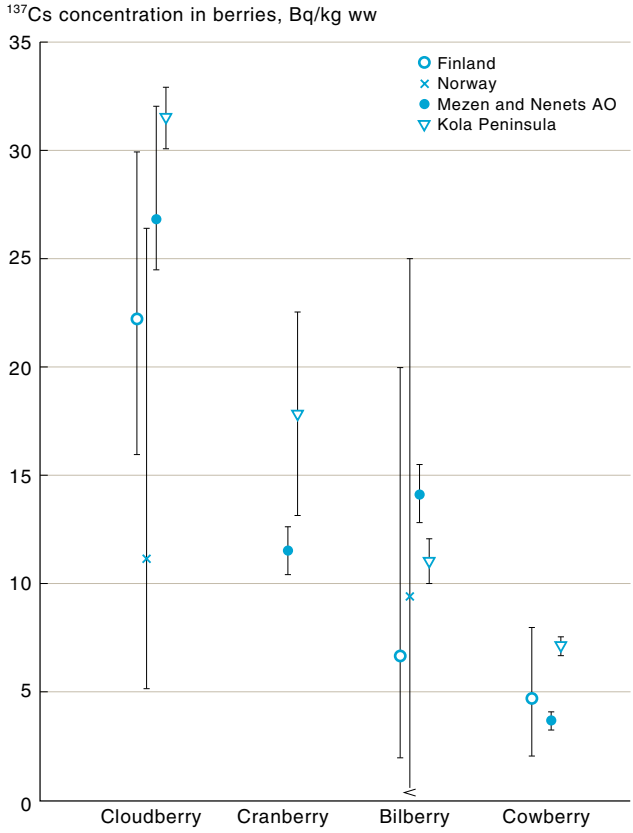

Figure 3·21. Activity concentrations of ^{137}Cs in berries from 1998 and 1999. Russian data: mean ± SD. Finnish and Norwegian data: mean and range. < : Under detection limit.

The Finnish, Russian, and Norwegian data are compared in Figure 3·21. Overall, the data indicate that cloudberry, which is a species typical of Arctic ecosystems, has the highest ^{137}Cs activity concentrations and is relatively vulnerable to radiocesium deposition compared to the other berry species. Cloudberry (and cranberry; *Vaccinium oxycoccus*) grow on wet, highly organic bogs, conditions which would be expected to lead to high radiocesium plant uptake from soil. Bilberry and cowberry grow on dry land, mainly in forests, in which the depth of the organic layer varies and sand is often present under the upper organic horizons.

The limited Finnish data suggest that the reduction with time in the ^{137}Cs content of Arctic berries is slow.

3.5.4. Milk

Sufficient data are now available on ^{137}Cs activity concentrations in milk to report on changes over time during the period of global fallout and after the Chernobyl accident for several locations in Finland, Sweden (annual averages), the Faroe Islands, Iceland, Russia, and Norway. The sample sites are shown in Figure 3·22. For ^{137}Cs, all time series show a peak in activity concentrations in the early-1960s with nearly 100 Bq/L detected in the Faroe Islands and Iceland. After the Chernobyl accident, some fallout was detected in milk in parts of Sweden, Arctic Finland, northern Norway, northwest Russia, and the Faroe Islands, with peak values of up to 20 Bq/L.

In most time series with an adequate sampling frequency, a strong seasonal signal can be seen with higher ^{137}Cs activity concentrations in the summer, when cows are put out to pasture or fed fresh grass. In some cases, the completeness of directly comparable time series has been affected by dairies closing down and consequent changes in the collection areas for those remaining.

Long-term time series on ^{90}Sr activity concentrations in milk are available for northern Finland, Sweden, Norway, and the Faroe Islands. Peak ^{90}Sr activity concentrations in the late-1960s were around 2 Bq/L in Fennoscandia. Little input from the Chernobyl accident was detected, although the weighted mean value in Sweden for ^{90}Sr in milk increased marginally from 0.10 Bq/L just before the Chernobyl accident to 0.13 Bq/L just after. In all time series with adequate sample numbers, a strong

Figure 3·22. Sites at which milk samples were collected.

seasonal signal in ^{90}Sr activity concentrations is seen with higher values in the summer.

The ^{137}Cs and ^{90}Sr activity concentration data are summarized in Table 3·9. Despite more ^{90}Sr being deposited during the period of global fallout, there were consistently higher ^{137}Cs activity concentrations in milk due to a roughly 15-fold higher transfer of ^{137}Cs to milk compared to ^{90}Sr.

3.5.4.1. Finland

Milk has been sampled at several sites in Finnish Lapland since the 1960s. Sampling was undertaken from 1963 to 1987 in Kursu, an area with boggy soils. Samples of milk powder were collected from a dairy in Rovaniemi from 1966 to 1975 and dairy milk from 1986 onwards. Samples from individual farms were collected from Apukka from 1975 to 1977 and 1986 to 1991 and from Vikajärvi from 1991 onwards. Kostiainen and Rissanen (2003) summarized the findings as follows: '*The highest ^{90}Sr and ^{137}Cs concentrations in the 1960s in Finnish milk were recorded in Lapland even though the deposition of ^{90}Sr and ^{137}Cs was no greater than in the rest of Finland. This was mainly due to the high proportion of peat soils and nutrient deficiency of the pastures in Lapland. Cs-137 deposition after the Chernobyl accident in 1986 in Lapland was less than 1 kBq/m^2, and ^{90}Sr deposition was so low that there was no detectable increase in the ^{90}Sr concentration in milk*.'

Although total ^{137}Cs deposition from nuclear weapons tests was similar in parts of Finland Lapland to that for Chernobyl fallout, ^{137}Cs activity concentrations in milk during the 1960s were considerably higher than after the Chernobyl accident. The pre-Chernobyl fallout, characterized by an annual maximum in summer, resulted in significant direct contamination of growing crops, whereas the Chernobyl deposition occurred before the start of the growing season in Lapland. The direct contamination of growing crops resulted in higher contamination levels compared to the short-term deposition following the Chernobyl accident when, before the start of the growing season, the food chain is hay to milk. The

Table 3·9. Activity concentrations for ^{137}Cs and ^{90}Sr in milk (Bq/L; mean (range)) (AMAP Data Centre).

		1964	1986	1998
^{137}Cs	Faroe Islands	51 (22-97)	5.8 (0.9-19)	0.8 (0.2-1.9)
	Arctic Finland	31 (27-36)	2.4 (0.5-5.2)	0.55 (0.5-0.6)
	Iceland	27 (7-83)	–	1.4 (0.9-2.4)
	Arctic Norway	16 (7-37)	6.2 (1-20)	–
	NW Arctic Russia	–	6.4 (4.0-10)	1.3 (0.04-0.3)
	Arctic Sweden	22 (14-30)	6.0 (2.0-13)	2.5 (1.5-4)
^{90}Sr	Faroe Islands	7.2 (3.3-12)*	–	0.04 (0.04-0.05)*
	Arctic Finland	1.1 (0.9-1.4)	–	0.05 (0.04-0.05)
	Iceland	–	–	–
	Arctic Norway	1.7 (1.3-2.2)	–	–
	NW Arctic Russia	–	–	0.17 (0.05-0.54)
	Arctic Sweden	1.4 (1.0-1.8)**	–	0.06 (0.03-0.09)

* the Faroese ^{90}Sr data were calculated from values in Bq/kg Ca, using an average of 1.2 g Ca in 1 kg milk;

** data from 1965, for Sweden, on average, ^{90}Sr levels declined by 18% from 1964 to 1965.

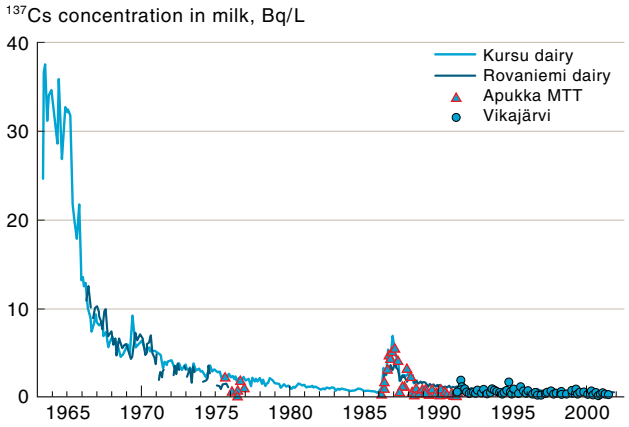

Figure 3·23. Time series for ^{137}Cs activity concentrations in milk from sites in northern Finland (Kostiainen and Rissanen, 2003).

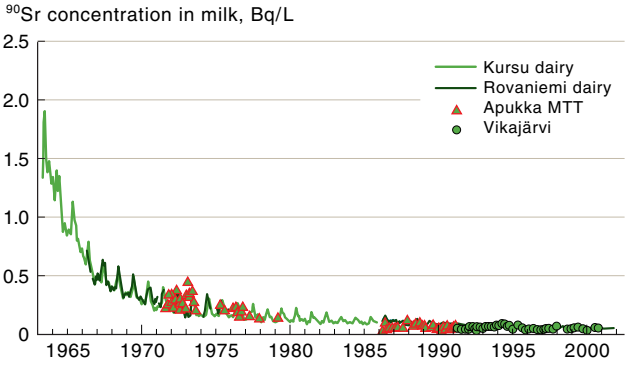

Figure 3·24. Time series for ^{90}Sr activity concentrations in milk from sites in northern Finland (Kostiainen and Rissanen, 2003).

time trends in ^{137}Cs and ^{90}Sr activity concentrations in milk are shown in Figures 3·23 and 3·24, respectively.

The increase in the activity concentrations of ^{137}Cs in milk due to the Chernobyl fallout was clearly visible in July 1986, and the peak lasted until summer 1987. In early-1987, activity concentrations in Kursu dairy milk were twice as high (5 to 7 Bq/L) as those from the Rovaniemi dairy (3.5 Bq/L), which collects milk from most of Lapland. The difference was due to the high frequency of peat soils and to the higher fallout in the area of the Kursu dairy compared to the average deposition in Lapland. The peak activity concentrations in the Apukka farm milk were about the same as in Kursu dairy milk, and decreased after summer 1988 to below the level of the Rovaniemi dairy milk. The activity concentrations of ^{137}Cs in Vikajärvi farm milk were similar to those in Rovaniemi dairy milk.

In contrast, ^{90}Sr in milk in Lapland is mainly from the fallout from nuclear weapons tests and the activity concentrations in milk from different areas of northern Finland were similar.

After the period of nuclear weapons tests, fallout continued to be deposited at lower, but not negligible levels, for several years. The T_{eff} values for ^{137}Cs and ^{90}Sr in milk after the peak values in 1963 were similar, at 2 yr in 1963 to 1966 and 5 yr in 1966 to 1975 (Table 3·10). During 1975 to 1985, the effective half-life of ^{137}Cs was still 5 yr, but for ^{90}Sr had increased to 10 yr. The effective half-lives of ^{137}Cs in milk after the peak concentrations resulting from the Chernobyl accident were similar to those in the 1960s to 1970s. The effective half-lives for ^{137}Cs in dairy milk and farm milk were about the same during the 1990s (at 7 to 8 yr), as were those for ^{90}Sr during the 1970s. There were larger fluctuations in the monthly activity concentrations of ^{137}Cs in farm milk than in dairy milk.

Table 3·10. T_{eff} values (yr) for ^{137}Cs and ^{90}Sr in milk at the Kursu and Rovaniemi dairies after the period of global fallout and the Chernobyl accident (Kostiainen and Rissanen, 2003).

	^{137}Cs		^{90}Sr	
	Kursu	Rovaniemi	Kursu	Rovaniemi
1963 to 1966	2.0		2.2	
1966 to 1975	4.8	3.2	5.1	6.1
1975 to 1985	5.3		10	
1987 to 1989		2.2		14
1989 to 1993		4.1		6.9
1993 to 2001		7.6		16

Kostiainen and Rissanen (2003) conclude that the whole of Lapland is vulnerable to radioactive contamination. The transfer of ^{137}Cs into milk from peat soils was more than twice that for the clay soils of southern Finland, and the T_{eff} values for milk in Lapland are twice those for intensively-cultivated clay pastures.

3.5.4.2. Sweden

Annual average ^{137}Cs activity concentrations at two sites in Arctic Sweden are shown in Figure 3·25. These indicate consistently higher values at Tärnaby than at Vittangi. A peak due to the Chernobyl accident can be seen in the values for Tärnaby milk.

A regular seasonal variation was evident for ^{137}Cs, and to a lesser degree for ^{90}Sr, during the 1950s and 1960s. Generally, peak levels occurred during the third quarter of the year coincident with the months of highest precipitation. Seasonal variations are especially pronounced in milk from the dairy in Tärnaby where cows graze in summer on natural pastures and in forests. A similar, but not as regular, seasonal variation was apparent after the Chernobyl accident.

T_{eff} values for ^{137}Cs in Swedish milk, estimated for the period from the peak of the atmospheric testing fallout until the Chernobyl accident, exhibit a fast and a slow component. The $T_{eff\,1}$ values were 1.4 and 1.8 yr, and the $T_{eff\,2}$ values 9.1 and 6.2 yr for Tärnaby and Vittiangi, respectively. The $T_{eff\,2}$ of 9.1 yr for Tärnaby is the longest $T_{eff\,2}$ for milk found in this study, but is not significantly longer than $T_{eff\,2}$ values found in northern Norway and on the Faroe Islands. Insufficient data were available to calculate post-Chernobyl T_{eff} values.

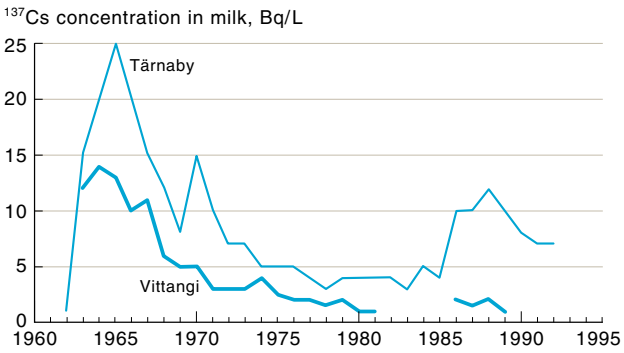

Figure 3·25. Annual average ^{137}Cs activity concentrations in milk for two sites in northern Sweden.

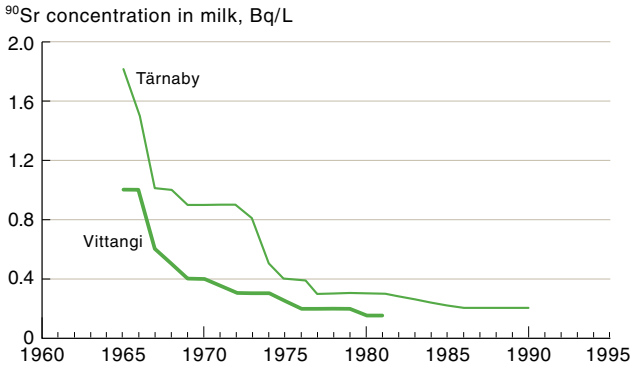

Figure 3·26. Annual average ^{90}Sr activity concentrations in milk for two sites in northern Sweden.

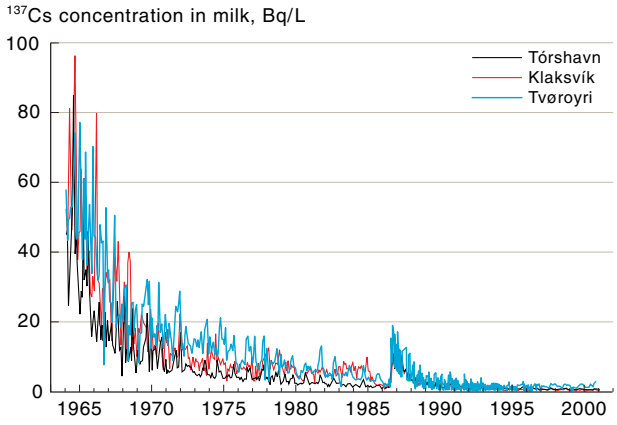

Figure 3·27. Weekly ^{137}Cs activity concentrations in milk at three locations in the Faroe Islands.

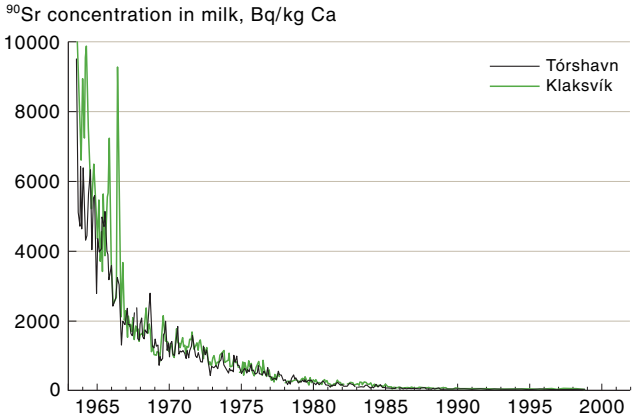

Figure 3·28. Weekly ^{90}Sr activity concentrations in milk (per kg Ca) from two sites in the Faroe Islands. The average calcium content of milk in the Faroe Islands is 1.2 g/L.

High precipitation combined with the high transfer of ^{137}Cs via the grass → cow food chain in natural pastures and forest environments was the main cause of the high activity concentrations and relatively slow decrease rates in milk at Tärnaby.

Annual average ^{90}Sr activity concentrations at the two sites in Arctic Sweden are shown in Figure 3·26. Again, consistently higher values occurred at Tärnaby than Vittangi. For ^{90}Sr, the short component (T_{eff1}) after 1963 was 2.1 yr, while the longer component (T_{eff2}) before and after the Chernobyl accident was 9.1 and 9.2 yr, respectively.

3.5.4.3. Faroe Islands

Milk has been sampled weekly in Tórshavn, Klaksvík, and Tvøroyri. The Klaksvík and Tvøroyri samples are from locally produced milk, while the Tórshavn samples are from a dairy which collects milk from most of the country. The ^{137}Cs activity concentrations are shown in Figure 3·27.

The T_{eff} for ^{137}Cs in milk from the Faroe Islands has been calculated to 6.5 to 8.8 yr for the long (second) component in global fallout, whereas the short (first) component was between 1.0 and 1.8 yr. For Chernobyl fallout, the T_{eff} was from 1.3 to 1.8 yr.

Activity concentrations of ^{90}Sr in milk have been measured as Bq/kg Ca (Figure 3·28). With an average Ca concentration of 1.2 g/L, the peak values of ~10000 Bq/kg Ca correspond to ~12 Bq/L. The short and long components in the T_{eff} for ^{90}Sr were found to be 1.1 to 1.4 and 5.2 to 5.5 years, respectively.

3.5.4.4. Iceland

The ^{137}Cs activity concentrations in Icelandic milk in the mid-1960s are shown in Figure 3·29. The average T_{eff} for ^{137}Cs in milk from these dairies during 1964 to 1967 was 3.0 yr, similar to that in Kursu in northern Finland. Soon after this period, the rate of reduction of Cs con-

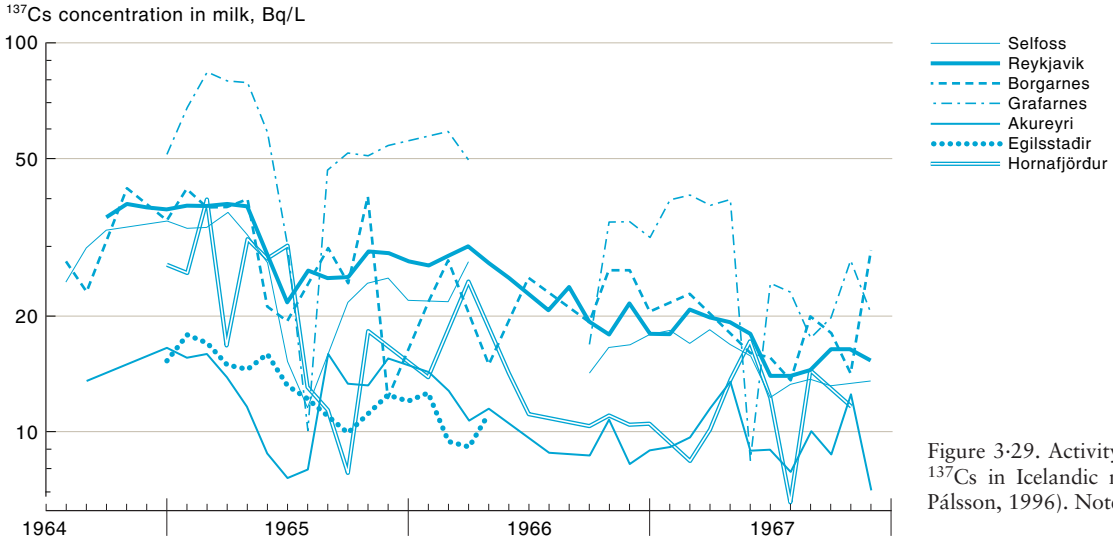

Figure 3·29. Activity concentrations for ^{137}Cs in Icelandic milk (adapted from Pálsson, 1996). Note logarithmic scale.

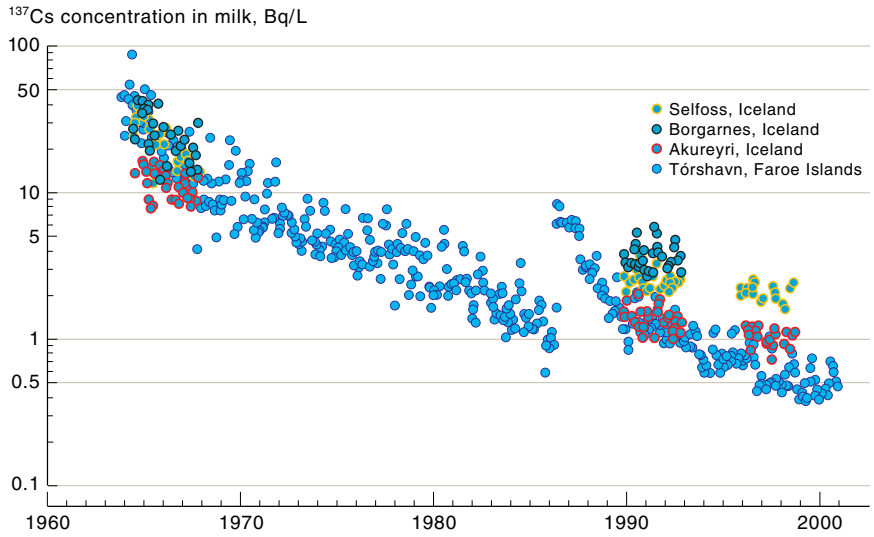

Figure 3·30. A comparison of ^{137}Cs activity concentrations in Icelandic and Faroe Island milk.

centration in milk decreased. The Icelandic data exhibit a high spatial variability between sample areas, with relatively high maxima compared to other Arctic areas. In particular, the values at Grafarnes are relatively high for many years although there are occasional dips. A comparison with the ^{137}Cs deposition map in Section 3.7.2.2 (Figure 3·52) shows good agreement between the pattern of deposition and ^{137}Cs activity concentrations in milk, with the highest values in the southwest and the lowest in the north.

Activity concentrations of ^{137}Cs in Icelandic (Selfoss, Borgarnes, and Akureyri) and Faroe Island (Tórshavn) milk are compared in Figure 3·30. This shows that activity concentrations in milk in the 1960s were slightly lower in Iceland than the Faroe Islands. However, in the 1990s, the levels in Iceland were higher in the three study areas than in Tórshavn, although the relative difference in concentration between the milk from the three Icelandic regions remained the same (Pálsson *et al.*, 2002b). This is despite the Faroe Islands receiving some fallout from the Chernobyl accident (see Figure 3·30), in contrast to Iceland where it was hardly detectable. The comparison indicates that the reduction in ^{137}Cs activity concentrations in milk has been slower in Iceland than the Faroe Islands. This is also reflected in the lower slope of the Icelandic data sets during the 1990s. The explanation may lie in the lower cesium-binding properties of the young volcanic Icelandic soils compared to those of the Faroe Islands (Sigurgeirsson *et al.*, 2002). It is thus concluded, as was also the case for Lapland, that Iceland is vulnerable to radioactive contamination due to high transfer of ^{137}Cs from soil to milk and very high T_{eff} values.

3.5.4.5. Norway

Figures 3·31 and 3·32 show ^{137}Cs and ^{90}Sr activity concentrations in milk from four dairies in Arctic Norway, since 1960. Because precipitation in Arctic Norway is low compared to precipitation on the southwest coasts, the deposition of global fallout in Arctic Norway is also relatively low compared to other parts of the country. In general, the spatial variation in activity concentrations broadly follows that for precipitation and therefore global fallout. The highest values were measured at Bodø, a coastal area. However, there is an anomaly in that levels at Kautokeino are higher than would be expected from the low rate of precipitation in this area. A possible explanation is that cows in Kautokeino were fed lichen as fodder (Eikelmann, pers. comm., 2002).

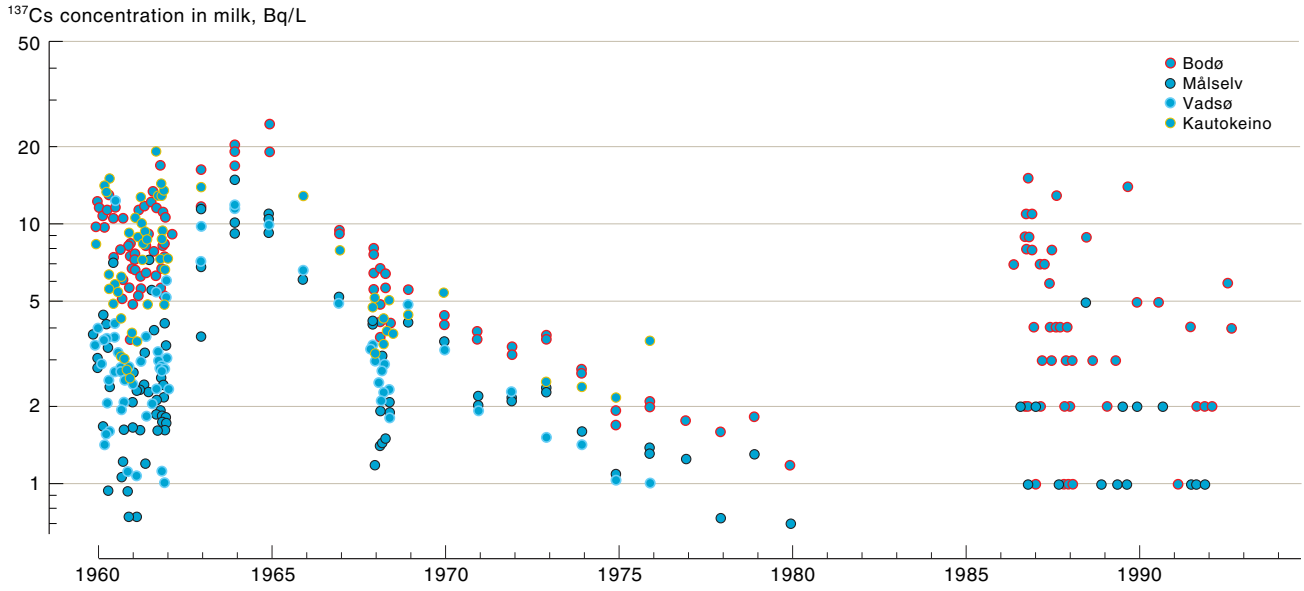

Figure 3·31. Activity concentrations of ^{137}Cs in milk at four locations in northern Norway.

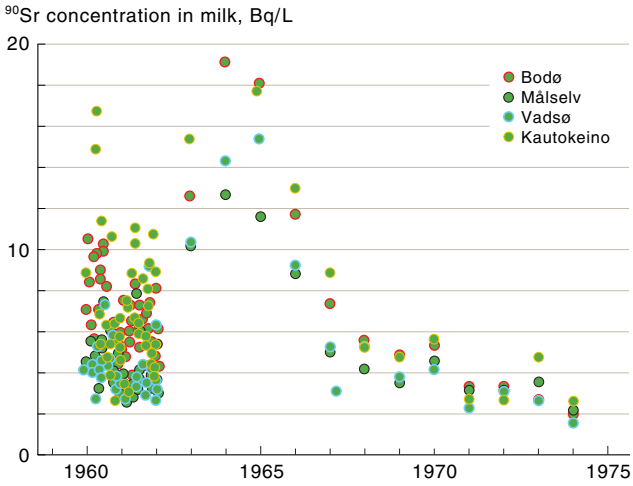

Figure 3·32. Activity concentrations of ^{90}Sr in milk at four locations in northern Norway.

The impact of the Chernobyl accident is variable, with fallout most noticeable at Bodø.

3.5.4.6. Russia

Sporadic data on ^{137}Cs activity concentrations in Russian milk from 1986 onwards support the findings in sections 3.5.4.1. to 3.5.4.5. Due to the limited amount of data available for milk in the Russian Arctic, a detailed assessment is not possible.

3.5.4.7. Trends

The data in sections 3.5.4.1 to 3.5.4.6 were collected using various techniques over different periods of time, which makes direct comparisons difficult. Nevertheless, a rough comparison between countries is attempted in Table 3·11 using double exponential T_{eff} values and a consistent method for the various sites in the different countries. All the half-lives were calculated using the statistical package 'R', and its nls- (nonlinear least squares) library. The T_{eff} values are estimated for global fallout data from 1964 to 1985, and for Chernobyl fallout from 1986 onward. The global fallout values are expected to be greater than for a single pulse input as global fallout continued to be deposited after the peak values in the mid-1960s.

A comparison of ^{137}Cs activity concentrations in milk from a range of locations in northern Scandinavia and the Faroe Islands in 1964, the year for which most data were available, shows that even though some samples came from dairies taking milk from a wide geographical area, a relationship is still evident between milk contamination and global fallout, which is linked to precipitation rates (Figure 3·33). Thus, for instance, within Norway and Iceland the west coast, which receives the highest rate of precipitation, produced the most contaminated milk. Some of the lowest values were recorded in the areas of Norway closest to the Novaya Zemlya test site.

Table 3·11. T_{eff} values (yr ± SD) for ^{137}Cs and ^{90}Sr activity concentrations in milk from various Arctic areas.

	Faroe Islands			Finland			Norway				Sweden	
	Klaksvík	Tórshavn	Tvøroyri	Apukka	Kursu	Rovaniemi	Bodø	Vadsø	Målselv	Kautokeino	Tärnaby	Vittiangi
^{137}Cs												
Global fallout												
T_{eff_1}	1.5±0.1	1.0±0.1	1.8±0.2		1.0±0.1		1.9±0.6	1.6±0.4	1.5±0.3	1.1±0.3	1.4±0.4	1.8±0.6
T_{eff_2}	7.1±0.5	6.5±0.4	8.8±0.7		4.5±0.7		4.5±1.2	5.1±1.3	6.1±1.2	6.0±2.0	9.1±1.1	6.2±1.0
Chernobyl fallout												
T_{eff}	1.3±0.1	1.8±0.1	1.8±0.1	0.7±0.1		3.4±0.1						
^{90}Sr												
T_{eff_1}	1.0±0.1	1.4±0.1			1.3±0.1		1.8±0.6	n.a.	n.a.	1.5±0.4	3.0±1.0	1.4±0.3
T_{eff_2}	5.2±0.4	5.5±0.5			8.4±0.3		4.0±1.0	n.a.	n.a.	4.6±1.3	9.0±2.0	8.5±1.0

n.a.: no statistically valid half-life could be calculated.

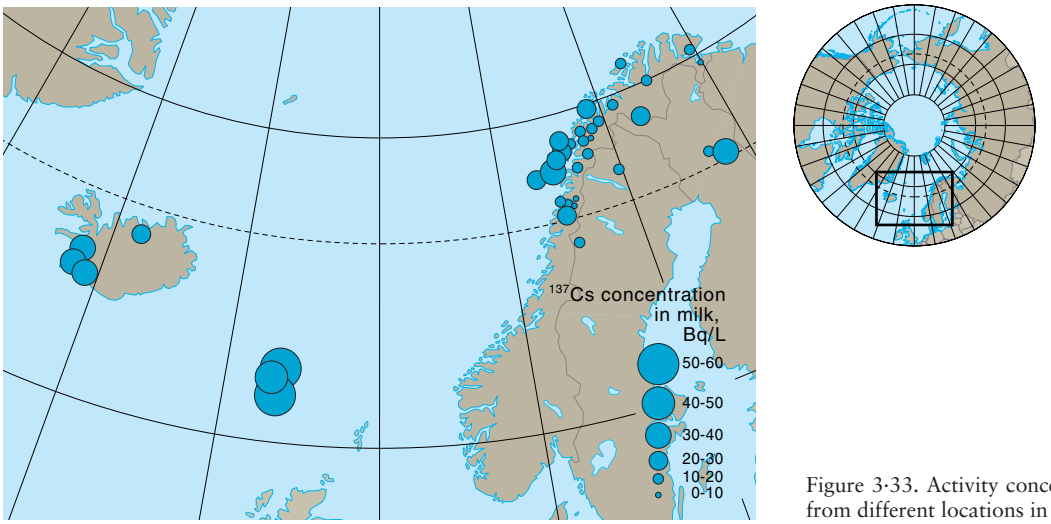

Figure 3·33. Activity concentrations of ^{137}Cs in milk from different locations in Nordic areas in 1964.

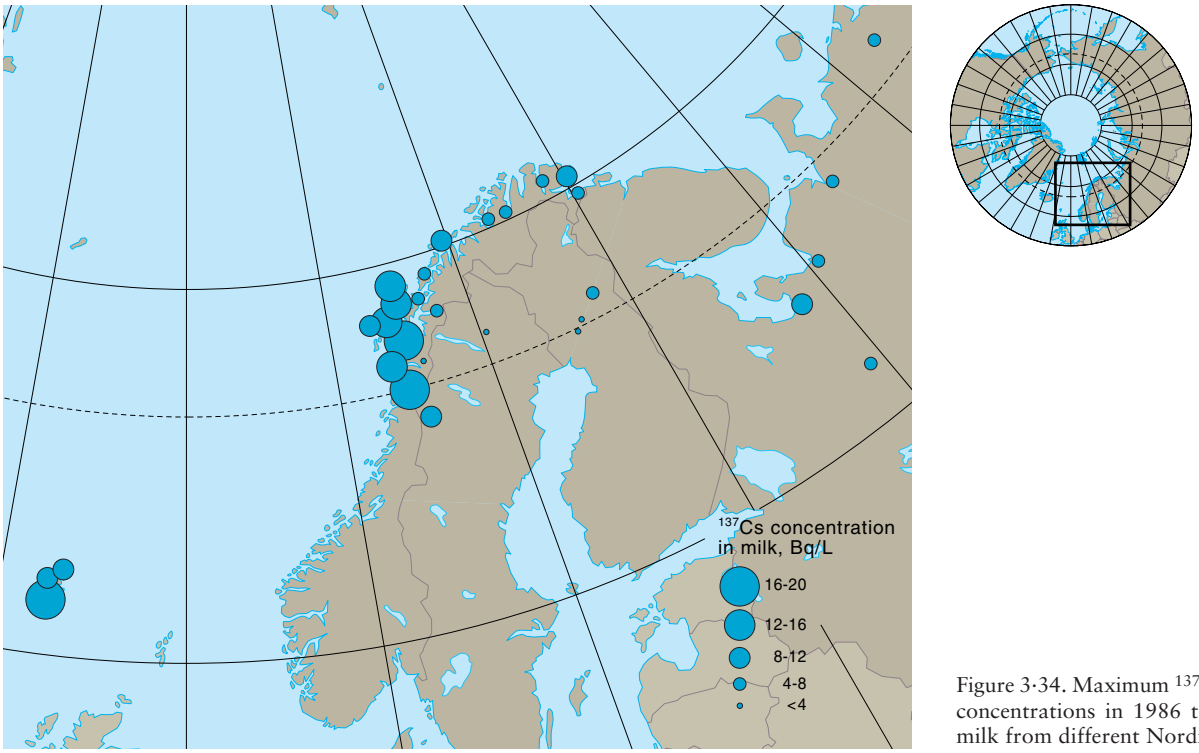

Figure 3·34. Maximum ^{137}Cs activity concentrations in 1986 to 1987 in milk from different Nordic areas.

The highest ^{137}Cs activity concentrations in milk, after the Chernobyl accident, are shown in Figure 3·34. In all Arctic areas, levels were higher in the global fallout period than after the Chernobyl accident.

There were no statistically significant differences in the average ^{137}Cs T_{ag} values from soil to milk (and beef) produced in two Russian Arctic regions (Table 3·12) after global fallout.

Table 3·12. ^{137}Cs T_{ag} values (10^{-3} m^2/kg) for beef and milk in northwest Russia (Borghuis *et al.*, 2002).

	n	Mean ± SD	*t*-test
Beef, 1978-1985			
Kola	7	0.28 ± 0.08	P = 0.10
Nenets AO	34	0.24 ± 0.12	
Milk, 1974-1978			
Kola	21	0.14 ± 0.07	P = 0.68
Nenets AO	7	0.12 ± 0.05	
Milk, 1978-1985			
Kola	12	0.082 ± 0.030	P = 0.081
Nenets AO	39	0.062 ± 0.035	

3.5.5. Lichen and reindeer

The long-term trend in ^{137}Cs activity concentrations in reindeer meat from the Kola Peninsula and the NAO region in Russia is shown in Figure 3·35. Over a 40-year period, the ^{137}Cs activity concentrations in meat from the Kola Peninsula were consistently statistically significantly higher than in the NAO region. One reason for the difference is the greater amount of global fallout on the Kola Peninsula than in the NAO region, but there may also be other contributory factors connected with pasture conditions.

Tables 3·13 and 3·14 present parameters describing the transfer and temporal variability in ^{137}Cs activity concentrations, such as T_{ag_0}, A_0, T_1, and T_2 (see Boxes 3·1 and 3·2), for lichen and reindeer meat, in northern Russia and northern Fennoscandia. These values are based on the assumption that the interception rate was the same for global fallout and Chernobyl fallout. Over the 40-year observation period, activity concentrations in lichen and reindeer meat are well described in all regions by a double exponential fit.

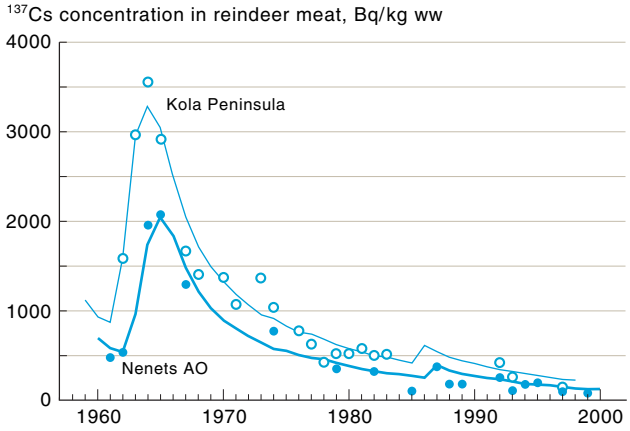

Figure 3·35. Changes with time in ^{137}Cs activity concentration in reindeer meat collected in the Kola Peninsula and NAO regions since 1961 (Borghuis *et al.*, 2002).

The T_{ag_0} values in Tables 3·13 and 3·14 were estimated on the basis of annual data. However, significant seasonal fluctuations are possible. Thus, for example, if the deposition in winter occurs onto snow, lichen is contaminated during the period of snowmelt and the interception fraction decreases through runoff as part of the activity is lost in snowmelt. In contrast, for a single dry deposition event, the interception fraction can be much higher than the annual mean value. Annual T_{ag_0} values must therefore be used with care as they are likely to underestimate single pulse deposition and do not take seasonal variation or (wet versus dry) deposition conditions into account.

Table 3·13. Initial values of the aggregated transfer coefficient (m^2/yr), ecological half-lives (T_{ec}, yr), and effective ecological half-lives (T_{eff}, yr) for ^{137}Cs and ^{90}Sr in lichen (dw). a is a parameter partitioning the decay between the two half-lives (see Box 3·1 and Box 3·2)

		T_{ag0}	a_1	T_{ec1}	T_{ec2}	T_{eff1}	T_{eff2}
^{137}Cs	Kola Peninsula	1.4	0.80	2.0	20	1.9	12
	Northern Sweden	1.4	0.52	3.4	14	3.0	10
^{90}Sr	Kola Peninsula	0.7	0.72	0.70	20	0.7	12

Table 3·14. Initial values of the aggregated transfer coefficient (m^2/yr), ecological half-lives (yr), and effective ecological half-lives (yr) for ^{137}Cs activity concentrations in reindeer meat (ww).

	T_{ag0}	a_1	T_{ec1}	T_{ec2}	T_{eff1}	T_{eff2}
Kola Peninsula	1.7	0.82	2.0	18	1.9	11
Nenets AO	1.2	0.81	1.8	15.6	1.5	10
Kautokeino (Norway)	1.8	0.83	1.2	13	1.1	9.0

Activity concentrations of ^{137}Cs in reindeer meat also vary over the year due to changes in food selection. In summer, reindeer eat herbaceous vegetation. In autumn they can eat large quantities of mushrooms. In winter, they mainly eat ground and arboreal lichens, which have a higher radiocesium content than herbaceous vegetation which they dig out from under the snow. The high interception of radionuclides by lichen, particularly radiocesium, is one of the key factors contributing to the most vulnerable Arctic food pathway, lichen → reindeer → man (Figures 3·36 and 3·37; Åhman and Nylén, 1998).

If contamination occurs during deep snow cover, then reindeer will ingest contaminated snow. The extent of intake is determined by the amount of snow ingested, but also by further snowfalls that may be less contaminated. The extent of contamination received from lichen depends on whether the contaminated snow overlying the lichen melts allowing the lichen to intercept the radioactivity. There can be a significant delay in reindeer attaining high levels of radiocesium from lichen owing to the protection of lichen by snow.

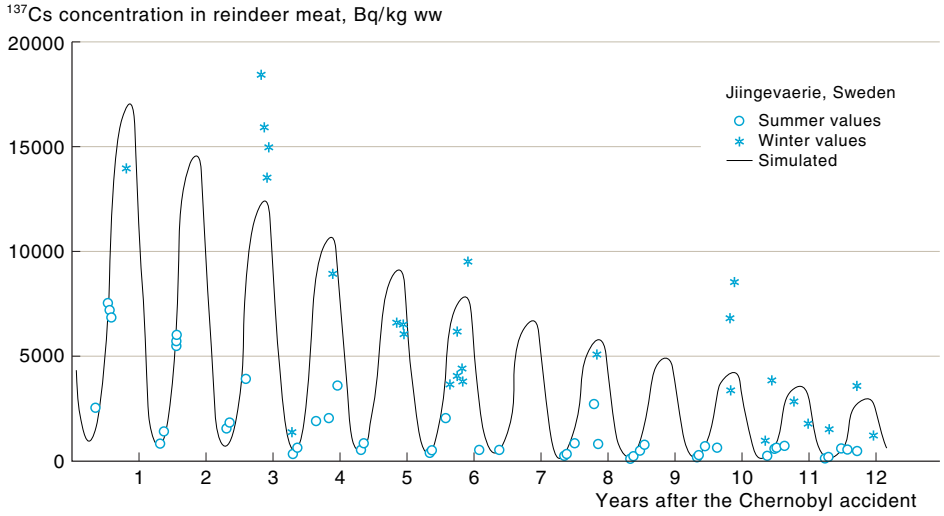

Figure 3·36. Activity concentrations of ^{137}Cs in fresh reindeer meat from the Jiingevaerie herding district in Sweden (Åhman and Nylén, 1998).

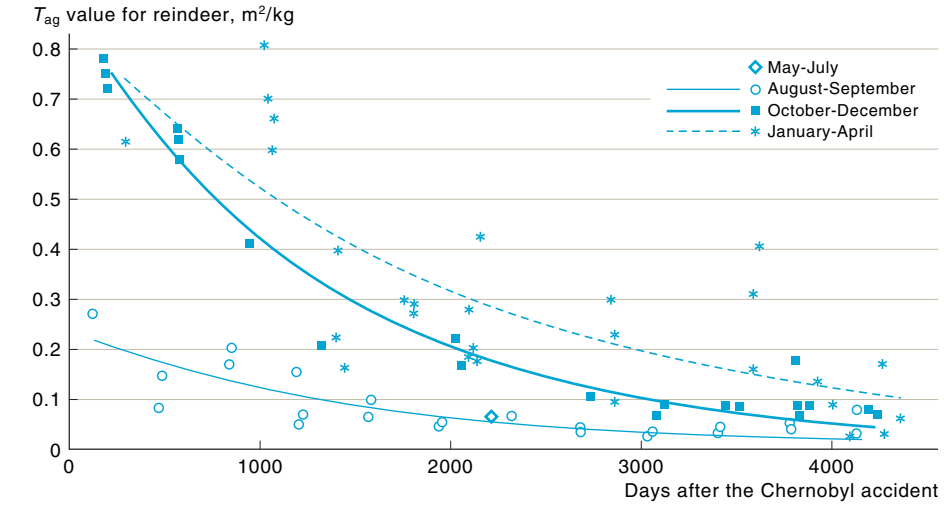

Figure 3·37. Seasonal variation in T_{ag} values for reindeer following the Chernobyl accident (Åhman and Nylén, 1998).

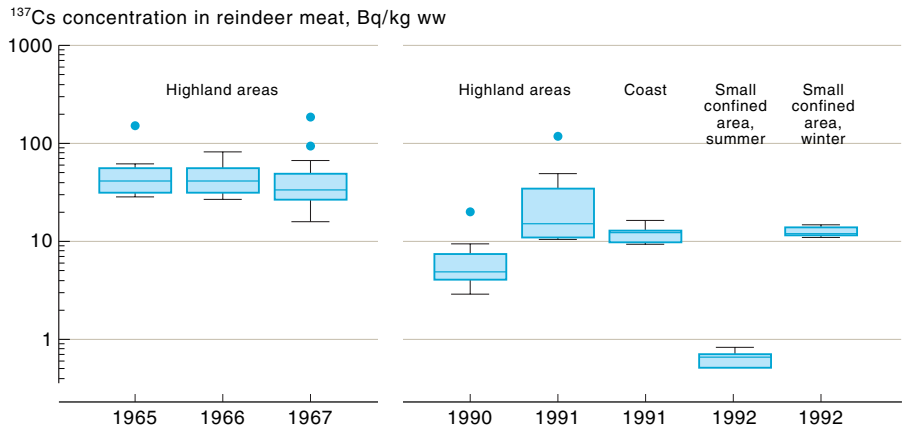

Figure 3·38. ^{137}Cs activity concentrations in meat from free-ranging reindeer from Iceland for different hunting seasons. Datasets for 1965 to 1991 are from highland areas and the coast, and the 1992 data from a more homogeneous restricted area.

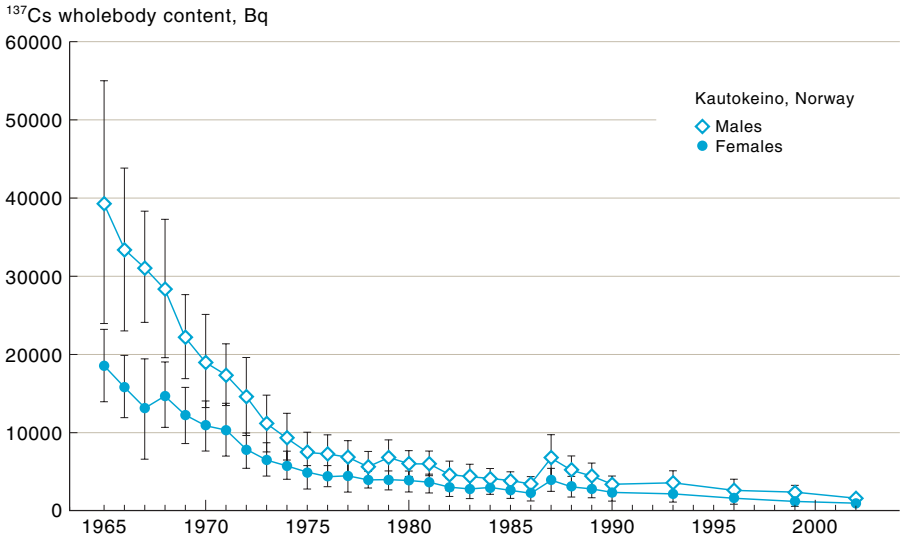

Figure 3·39. Wholebody measurements of ^{137}Cs in reindeer herders from Kautokeino, Norway.

Significant changes from year to year due to changes in food selection and variability in the ^{137}Cs activity concentrations in plants are also clearly visible in a study of wild free-ranging reindeer in Iceland. They are relatively few in number (around 3000) and roam within a highland region of different types of vegetation. A few samples were obtained each year by inspectors monitoring the hunting together with information about the location in which the animals had been shot and where they had grazed (Figure 3·38).

If the herd had grazed a large area with different types of vegetation, this was reflected in greater variability in the activity concentrations in the meat. If the herd had grazed a relatively small or uniform area, then activity concentrations showed little variability. The grazing areas selected by the herd varied from year to year, influenced for example by climate and the state of the vegetation. The lowest values (<1 Bq/kg ww) occurred in samples from 1992 from a herd that had grazed a relatively homogeneous area confined by glacial rivers and close to the glacier Vatnajökull.

3.6. Humans

Trends in wholebody measurements of ^{137}Cs presented in the first AMAP assessment have been extended by new data on wholebody measurements for northern Norway, Finland, and the Kola Peninsula and NAO regions of northwest Russia (see Table 3·15). An example of the temporal trend since 1965 is shown in Figure 3·39.

Table 3·15. Wholebody measurements (Bq) for reindeer herders (STUK; NRPA; Borghuis *et al.*, 2002).

		Males	Females	Average
Russia				
Kola	1999			3250±250
Finland				
Inari	1995			3300
	1997			3000
Norway				
Kautokeino	1996	2600±1400	1400±600	
	1999	2200±800	1100±400	
	2002	1414	872	

3.7. Site-specific data

3.7.1. Faroe Islands

The Faroe Islands were not addressed in the first AMAP radioactivity assessment. They comprise 18 islands between 6°15'W and 7°41'W and 61°20'N and 62°24'N with a total land surface area of 1399 km^2 (Figure 3·40). The land is mountainous, with the highest peak 882 m above sea level. There were 46 180 inhabitants on 31 December 2000. There is no woodland on the Faroe Islands. Land cover is dominated by rough, semi-natural pasture, and is grazed throughout the year by around 70 000 sheep and some cattle.

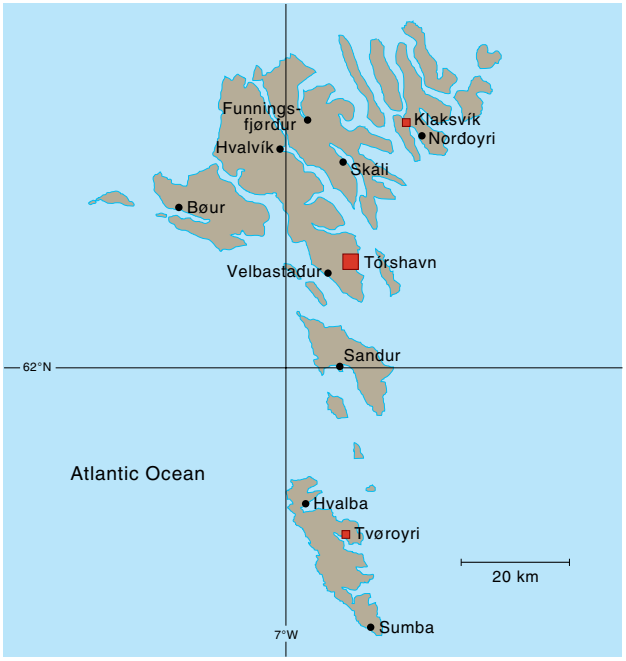

Figure 3·40. The Faroe Islands.

3.7.1.1. Climate

The climate is milder than might be expected at a latitude of 62°N due to the influence of the North Atlantic Current (the 'Gulf Stream'). Measurements at synoptic weather stations within 100 m of sea level, indicate an average annual air temperature of 6 to 7°C, with average winter and summer air temperatures of 3 to 4°C and 9 to 10°C, respectively (Cappelen and Laursen, 1998; Lysgaard, 1969). Only minor differences in air temperature occur between the synoptic stations. There is significant spatial variation in precipitation rates, however, due to the combined effects of meteorology and topography. These synoptic data are not totally representative of the Faroese climate however, as the zone within 100 m of sea level only covers 10% of land area. The climatic conditions change gradually from cool temperate oceanic conditions at the coast to Arctic conditions in the mountains (Mortensen, 2002). The annual average temperature at a new weather station on the mountain Sornfelli, 722 m above sea level, was 1.71°C in 2000 (Mortensen, 2002).

3.7.1.2. Cesium-137 and ^{90}Sr in precipitation and foodstuffs

Measurements of environmental radioactivity have been carried out on samples from the Faroe Islands since 1962, with an emphasis on terrestrial and marine foodstuffs.

Precipitation

Monthly precipitation samples have been obtained for radioactivity analyses since the 1960s. Annual average ^{137}Cs deposition rates in Tórshavn in the central part of the country and in Klaksvík in the north, shown in Figure 3·41, were highest in the early-1960s and showed a pronounced peak following the Chernobyl accident in 1986. Pre-1986 ^{137}Cs data are based on ^{90}Sr measurements (using a ^{137}Cs : ^{90}Sr fallout ratio of 1.6); after 1986 they are actual measurements (Figures 3·41 and 3·42).

Lamb meat

Figures 3·43 and 3·44 show annual average ^{137}Cs and ^{90}Sr activity concentrations in lamb meat, based on a few samples collected mainly in October. Trend analyses were not possible because the samples were collected from different places and there is significant spatial vari-

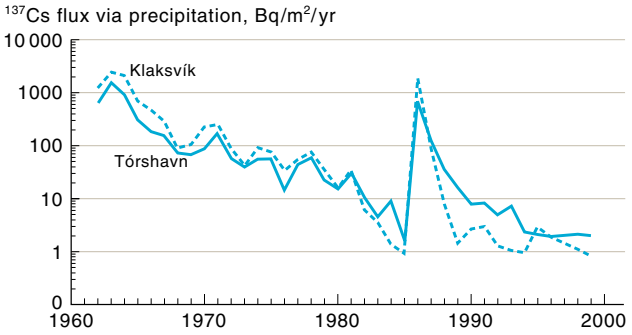

Figure 3·41. Annual average ^{137}Cs levels in precipitation from Tórshavn and Klaksvík, Faroe Islands.

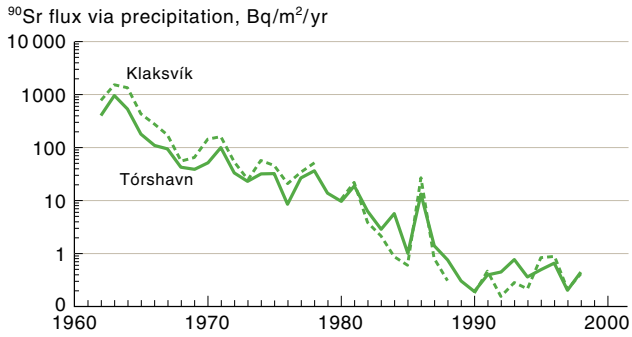

Figure 3·42. Activity concentrations of ^{90}Sr in precipitation from Tórshavn and Klaksvík, Faroe Islands.

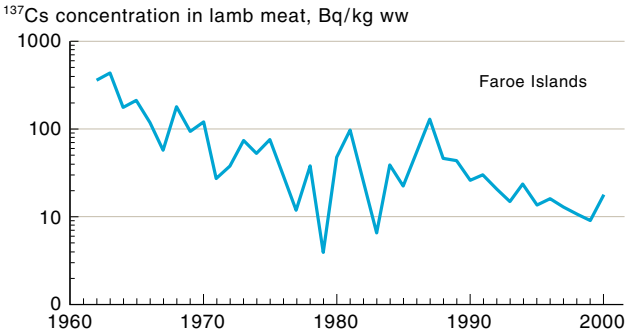

Figure 3·43. Annual average ^{137}Cs activity concentrations in lamb meat, Faroe Islands.

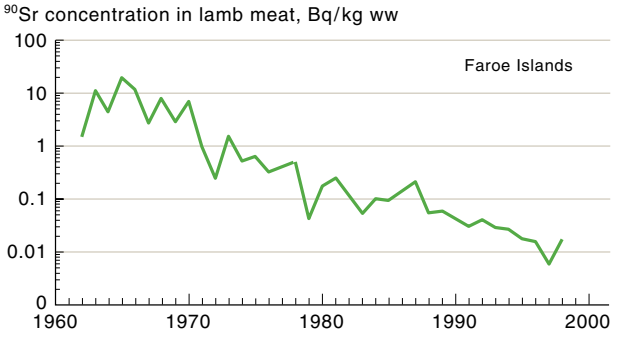

Figure 3·44. Annual average ^{90}Sr activity concentrations in lamb meat, Faroe Islands.

ation in contamination across the country (Joensen, 1999). During the 1990s however, the samples were collected consistently from the same places. Figure 3·43 indicates increased ^{137}Cs activity concentrations after the Chernobyl accident. In contrast, ^{90}Sr activity concentrations in lamb meat are lower and are not affected by Chernobyl fallout (Figure 3·44).

Drinking water

Figure 3·45 shows annual average activity concentrations for ^{90}Sr in tap water from Tórshavn and Klaksvík since 1962. Faroese drinking water is obtained from surface water. Sampling frequency has varied from monthly in the early-1960s to an annual summer value in the 1990s. No ^{90}Sr from Chernobyl was observed in drinking water.

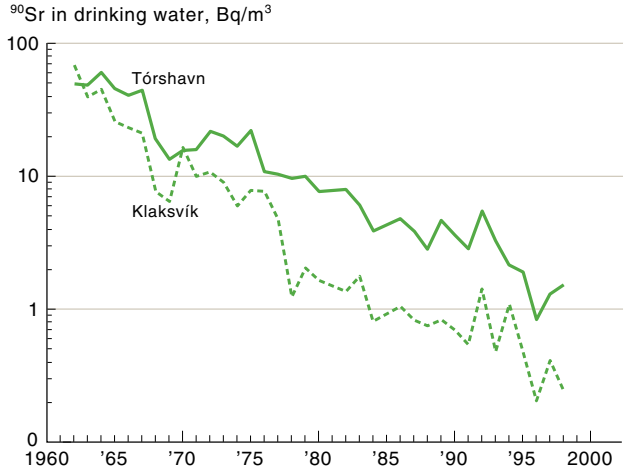

Figure 3·45. Annual average activity concentrations for ^{90}Sr in drinking water from Tórshavn and Klaksvík.

Effective ecological half-lives

Table 3·16 presents T_{eff} values for ^{137}Cs and ^{90}Sr in milk, lamb meat, precipitation, and drinking water. These are estimated by regressing the logarithm of the measured activities against time. The ^{137}Cs T_{eff} values in foodstuffs range from 4.9 to 8.7 yr, while those for ^{90}Sr range from 3.7 to 4.5 yr. Figures 3·41 to 3·45 and Table 3·16 indicate a tendency for increasing T_{eff} values with time. Despite the small geographical extent of the Faroe Islands, spatial variation in the T_{eff} values is apparent.

3.7.1.3. Transfer of ^{137}Cs within the lamb food chain in semi-natural pastures

Spatial variability in ^{137}Cs transfer to lamb has been evaluated by comparing its characteristics at nine uncultivated pastures during 1990 to 2000. Their locations are shown in Figure 3·40 (locations marked by black symbols). T_{eff} values and transfer factors for various components of the lamb food chain were estimated for the nine pastures. The soil at each site was previously characterized by Hove *et al.* (1994) and Joensen (1999).

Soil

There are large temporal and spatial variations within and between pastures in terms of ^{137}Cs deposition in the upper 10 cm soil layer (Figure 3·46). Between 50 and 80% of the deposition in this layer occurs in the upper 5 cm. Deposition ranges from 2000 to 8000 Bq/m^2. There was no consistent pattern of change with time for the nine pastures; with clear declines in some pastures, but not in others.

Soil pH in the nine pastures was between 4.4 and 5.3, and loss on ignition was 50 to 70% (Joensen, 1999). Thus these soils are acidic with a high organic matter content: conditions that favour a high uptake of radiocesium.

Grass

Activity concentrations of ^{137}Cs in mixed grass decreased in most pastures during the 1990s, with the highest levels in Hvalvík and the lowest in Hvalba. Although Figure 3·46 shows little clear difference in deposition between the nine sites, change over time in the grass varied widely (Figure 3·47). In some pastures early declines were evident, which were presumably due to the declining Chernobyl input, while others showed no overall decline, and others an approximate 20-fold decline.

Soil-to-grass T_{ag} values for the nine pastures are shown in Figure 3·48. The highest values occurred in Hvalvík and the lowest in Hvalba and Sandur. A multiple linear regression analysis between T_{ag} values and pH, loss on ignition, and potassium, showed loss on ignition to be the most significant factor (Joensen, 1999), and that the regression coefficient is negative for pH and potassium, and positive for loss on ignition. There were two orders of magnitude between the lowest and highest

Table 3·16. Estimated T_{eff} values (yr) based Figures 3.41 to 3.45. r^2 (shown in brackets) from linear regression of the natural logarithm of the measured activity concentrations against time.

		Milk	Lamb meat	Precipitation	Drinking water
^{137}Cs*	Klaksvík	6.2 (0.846)			
	Tórshavn	4.9 (0.959)			
	Tvøroyri	5.8 (0.971)			
	'Faroes'		5.5 (0.555)		
^{137}Cs**	Klaksvík	5.3 (0.980)		3.3 (0.940)	
	Tórshavn	6.4 (0.977)		4.3 (0.932)	
	Tvøroyri	7.1 (0.987)			
	'Faroes'		8.7 (0.772)		
^{90}Sr***	Klaksvík	4.4 (0.980)		2.8 (0.941)	5.1 (0.958)
	Tórshavn	4.4 (0.985)		3.2 (0.953)	6.9 (0.966)
	Tvøroyri	4.5 (0.986)			
	'Faroes'		3.7 (0.935)		

*only pre-Chernobyl data; **all data except for 1986 to 1992 (to avoid the Chernobyl peak); ***all data.

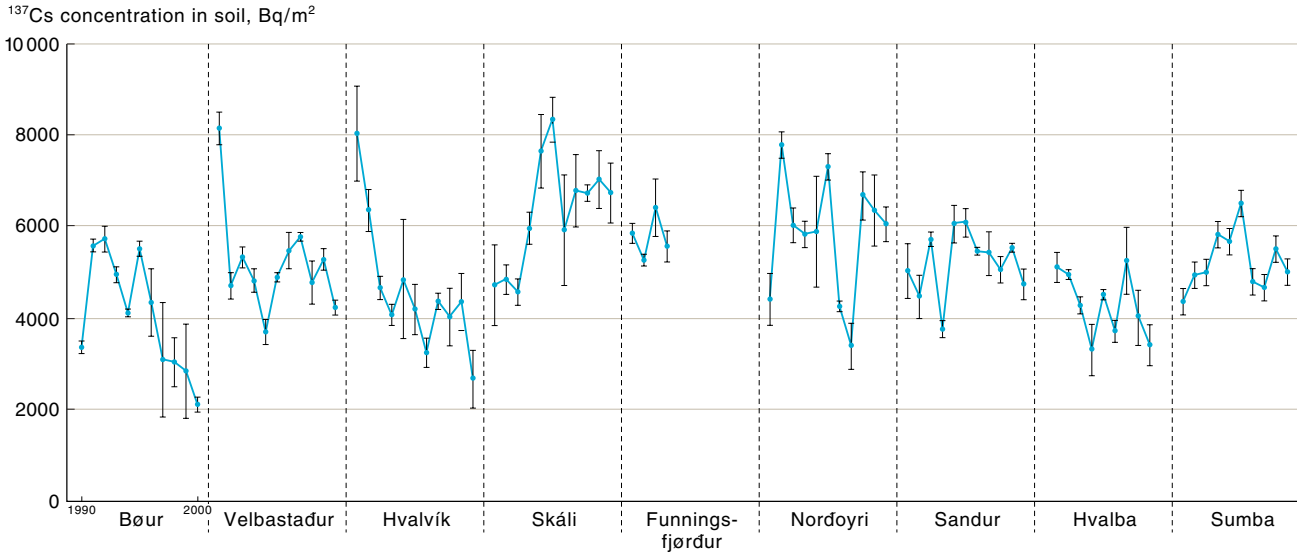

Figure 3·46. Annual average (±SE) ^{137}Cs deposition to surface soil (upper 10 cm) between 1990 and 2000 (1999 for Hvalba and Sumba) in the Faroe Islands (for locations see Figure 3.40).

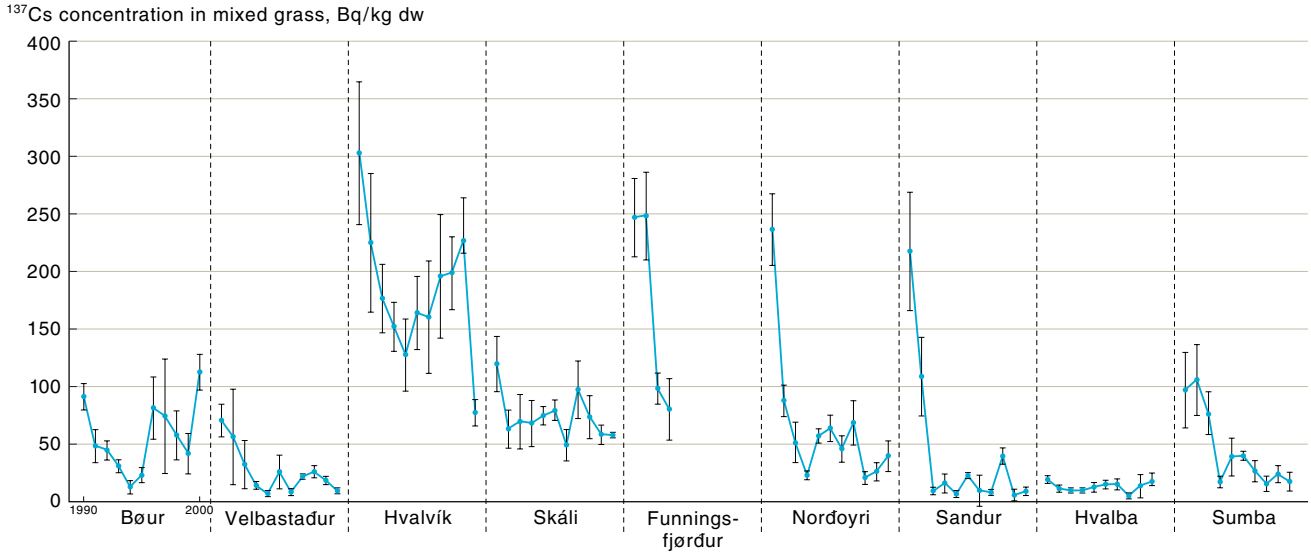

Figure 3·47. Annual average (±SE) ^{137}Cs activity concentrations in mixed grass between 1990 and 2000 (1999 for Hvalba and Sumba) in the Faroe Islands (for locations see Figure 3.40).

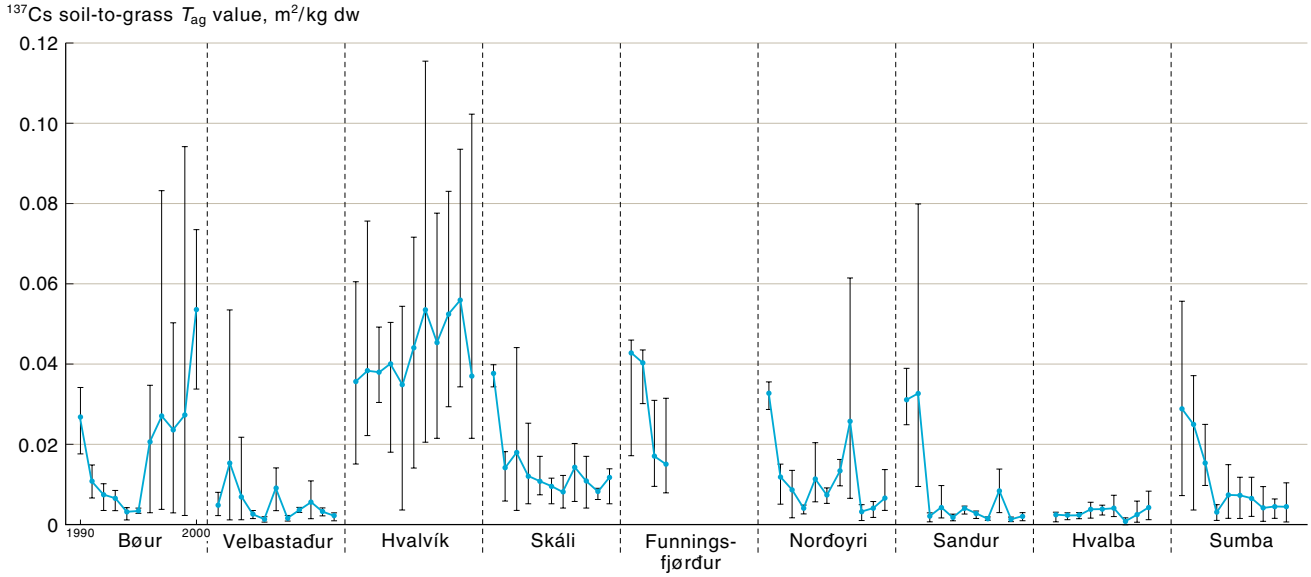

Figure 3·48. Annual average and ranges of soil-to-grass T_{ag} values for ^{137}Cs between 1990 and 2000 in the Faroe Islands (for locations see Figure 3.40).

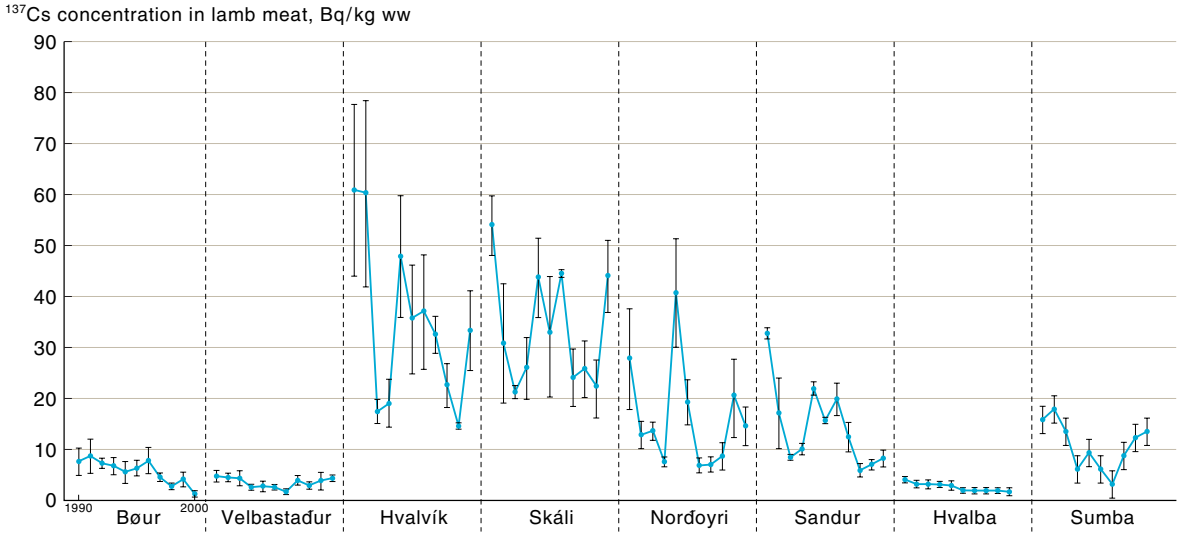

Figure 3·49. Annual average (±SE) ^{137}Cs activity concentrations in lamb meat between 1990 and 2000 (1999 for Hvalba and Sumba) in the Faroe Islands (for locations see Figure 3.40).

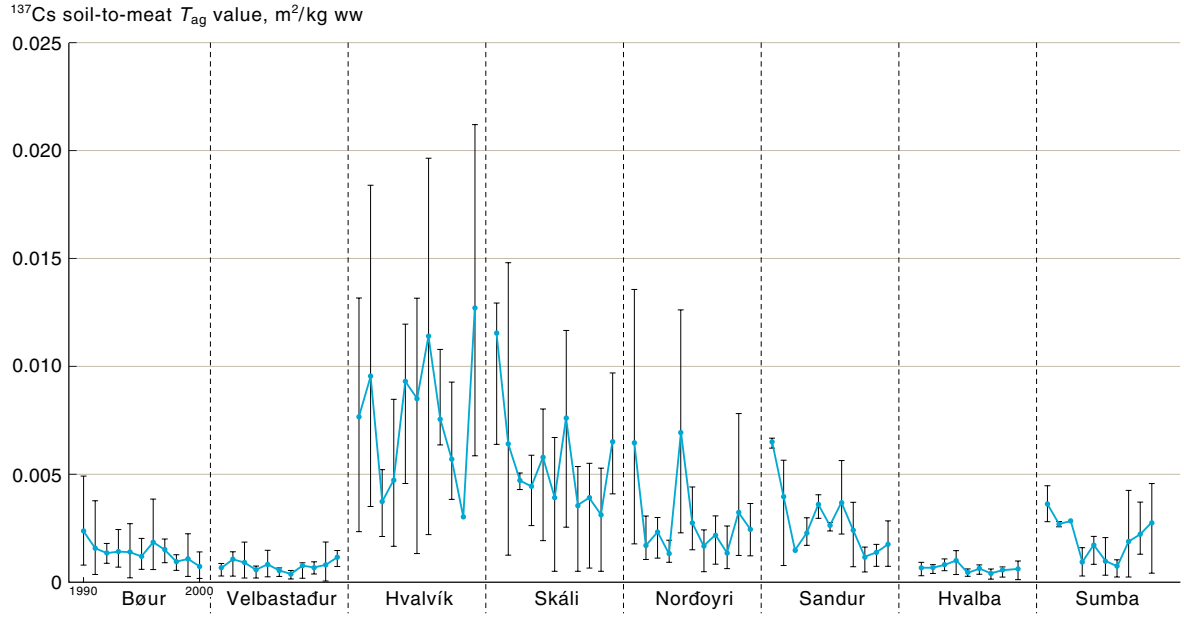

Figure 3·50. T_{ag} values for ^{137}Cs transfer to lamb meat at nine different sites in the Faroe Islands (for locations see Figure 3.40). Yearly averages and ranges 1990-2000.

T_{ag} values over the ten-year period. Some individual pastures showed a similar degree of variation. There was no clear time dependency in T_{ag} values at most sites.

Lamb meat

Figure 3·49 shows ^{137}Cs activity concentrations in lamb meat for 1990 to 1999. Large standard errors reflect large individual variation between animals. The highest values occurred at Hvalvík, Skáli, and Norðoyri.

The T_{ag} values at the nine sites are shown in Figure 3·50. Again, the highest values occurred at Hvalvík, Skáli, and Norðoyri. There is significant variation in T_{ag} values within and between sites.

Effective ecological half-lives

Effective ecological half-lives were derived for ^{137}Cs activity concentrations in grass and meat (Table 3·17). They could only be estimated for some pastures.

Table 3·17. T_{eff} values (yr) based on measurements for 1990 to 2000. r^2 (shown in brackets) from linear regression of the natural logarithm of the measured ^{137}Cs activity concentrations against time. No estimates given when $r^2 < 0.3$.

	Bøur	Velbastaður	Hvalvík	Skáli	Norðoyri	Sandur	Hvalba	Sumba
Grass	-	5.3	–	–	5.3	3.1	–	3.6
	(0.027)	(0.306)	(0.235)	(0.167)	(0.93)	(0.379)	(0.005)	(0.667)
Meat	5.1	–	–	–	–	6.9	8.0	–
	(0.668)	(0.033)	(0.199)	(0.031)	(0.060)	(0.392)	(0.873)	(0.069)

Conclusion

Even though the Faroe Islands cover a small geographical area, there was considerable spatial and temporal variation in the transfer of ^{137}Cs from soil to both grass and lamb meat. Owing to this high variability it is inappropriate to use a single T_{ag} value for either grass pasture or lamb meat. In other countries, there is generally greater variation in the key soil characteristics influencing radiocesium uptake than was measured at these sites. Even higher variability could thus be expected in other countries and country-wide generalizations about transfer are open to considerable error.

3.7.2. Iceland

3.7.2.1. Site description

Iceland is the second largest island in Europe, located in the North Atlantic just south of the Arctic Circle. The total surface area is 103 000 km^2, of which 23 805 km^2 (23%) are vegetated, 11 922 km^2 glaciers, 2757 km^2 lakes, and the remaining 64 538 km^2 (63%) barren. The coastline, including fjords and inlets, is about 4970 km long.

Iceland is the most sparsely populated country in Europe with an average of 2.8 inhabitants per km^2. On 31 December 2000 the number of inhabitants was 283 361.

The Icelandic diet is western European in most respects. Nevertheless it retains some characteristics of a subarctic region, making it unique among European nations. Fish, meat, and milk are traditionally the main foods produced in Iceland. Icelanders consume more fish than any other nation in Europe (73 g/d/cap) and, in general, food of animal origin constitutes a large proportion of the Icelandic diet. During the 1990s, the consumption of lamb meat decreased, beef consumption increased slightly, and the consumption of pork and poultry increased significantly (50 to 100%). This is reflected in agricultural production figures, since most of the products are consumed domestically.

In 2000, there were 466 000 sheep and 72 000 cattle on Iceland. During summer the sheep graze freely on rangelands in the interior, the same applies for a proportion of the 74 000 horses and around 4000 wild reindeer (*Rangifer tarandus*, the original herd imported from Scandinavia between 1771 and 1787) which inhabit the northeast of the country. Although reindeer constitute a minor part of the Icelandic diet, hunting is an increasingly popular sport, which also provides an important source of income for local communities.

Thus, sheep, horses, and reindeer would be affected by contamination of the highland areas of Iceland, whereas lowland contamination would affect cattle, and pig and chicken farming.

Volcanic eruptions are frequent in Iceland, producing lava fields and volcanic ash deposits of various extent. The unstable barren areas of the highlands and the floodplains of glacial rivers act as sources of aeolian material. The parent materials of Icelandic soils are largely of volcanic origin. Icelandic soils are mostly andosols, which are characterized by low cohesion and a high capacity to absorb water (>100% on a dry weight basis). This high water-holding capacity intensifies freezing effects, resulting in solifluction, landslides, needle ice formation, and the formation of hummocks (Arnalds, 1999).

The uneven surface of the rangeland areas and the sparse vegetation can make it difficult to obtain representative deposition estimates by sampling the soils.

The first AMAP assessment (AMAP, 1998) identified Iceland as one of the Arctic areas receiving the most fallout from atmospheric nuclear weapons tests, owing to relatively high precipitation rates compared with much of the rest of the Arctic and subarctic (Wright *et al.*, 1999).

The ^{137}Cs in the Icelandic terrestrial ecosystem originates almost entirely from nuclear weapons tests carried out in the atmosphere until the early-1960s. Fallout was greatest in the mid-1960s. Additional fallout from the Chernobyl accident was relatively small (Pálsson, 1996). This section provides data on radionuclide contamination in Iceland and uses recently acquired data to test the methodology and conclusions of the first AMAP assessment regarding global fallout.

Measurements of fallout from nuclear weapons tests in soil, vegetation, and agricultural products started in Iceland over 40 years ago (Pálsson, 1996). Considerable variability was present in the results, even between adjacent sites, probably due to the mountainous terrain, variable and strong winds, and highly variable levels of precipitation. This variability is particularly noticeable for soils. Early measurements of nuclear fallout were restricted to cultivated lowland areas. The importance of uncultivated rangelands in Icelandic agriculture (e.g., for sheep farming) makes their inclusion desirable for current and future estimates of radionuclide transfer into agricultural products.

Since summer 2000, spatial variation in ^{137}Cs deposition in Iceland has been studied systematically. The objectives of the study are to measure the spatial variation of radiocesium inventories in Icelandic soils and to compare the results with predicted ^{137}Cs soil levels (Sigurgeirsson *et al.*, 2002).

In summer 2000, soil samples were collected to a depth of 25 cm at 14 sites. The sites were located close to meteorological measurement stations so that representative precipitation data were available. Deposition at each site was estimated by assuming the ^{137}Cs activity concentration in precipitation was the same at all sites during any given period. Thus, deposition at each site is estimated by measuring the activity concentration of ^{137}Cs in precipitation at one reference site and then estimating deposition at the other sites by summing the product of precipitation (in m) at the site and ^{137}Cs in precipitation (in Bq/m^3) at the reference site for the period of interest (Pálsson *et al.*, 2002a,b).

A reference station close to Reykjavík (Rjúpnahæð, location 7 on Figures 3·51 and 3·52) was used for predicting fallout in Iceland, and quarterly measurements of fallout radioactivity in precipitation were undertaken regularly by the U.K. Atomic Energy Authority from 1959 to 1982 (Pálsson, 1996). Precipitation data for the reference site were supplied by the Icelandic Meteorological Office (Veðráttan 1959-1983). The reference station data show that 82.9% of the decay-corrected deposition of ^{137}Cs occurred during the first eight years, i.e., 1960 to 1967. The emphasis of the study was thus placed on meteorological stations that were operational during this eight-year period; estimates of deposition for these years were based on 1960 to 1967 precipitation data. The results were subsequently scaled up to cover the entire study

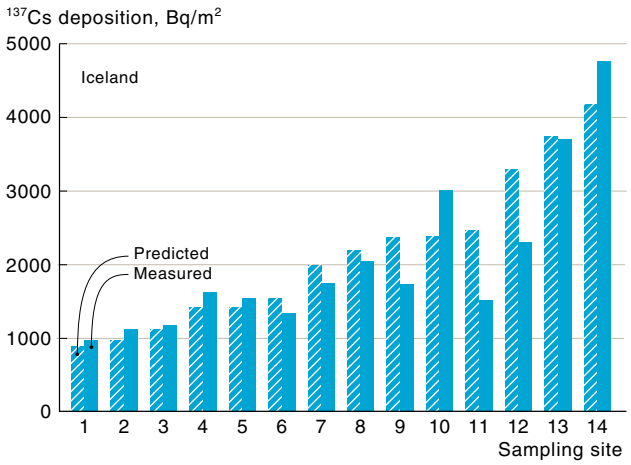

Figure 3·51. Comparison of predicted ^{137}Cs deposition based on precipitation data and measured values at fourteen sites (see Figure 3·52 for locations) close to meteorological stations in Iceland (Pálsson *et al.*, 2002a).

period, 1960 to 1982, assuming in all cases that 82.9% of the deposition had occurred during the first eight years used for calculations. Fallout data prior to 1960 were not included in this study and thus the measured values should be slightly higher than those predicted.

The measured ^{137}Cs content per unit area of soil varied from 900 to 4700 Bq/m^2, with deposition greater in the south of Iceland which receives more precipitation.

There are various ways of estimating the correlation between predicted and measured ^{137}Cs deposition. The method used in the comprehensive AMAP study (Wright *et al.*, 1999) was to force the regression line through the origin and calculate correlation coefficients on that basis. This gives a higher value for the correlation coefficient than for an unbound regression line, but can be justified in that the assumption being tested is that deposition is directly proportional to precipitation. This approach was used in the present study. Figure 3·51 compares measured and predicted deposition at the 14 sites.

The correlation between predicted and measured values for Iceland was much stronger than that reported by Wright *et al.* (1999). The AMAP study was based on 50 samples obtained from Greenland, Norway, and Russia between 1961 and 1985. A line through the origin was fitted to the data using least squares regression and gave an r^2 value of 0.51 based on a coarse precipitation data set and disparate sources of measured ^{137}Cs deposition using different sampling methods. In Iceland, a comparison of predicted and measured values gave a corresponding r^2 value of 0.96. This same value was obtained using both the AMAP method and when prediction was based on average annual precipitation for 1960 to 1967. Some of the improved correlation relative to the AMAP study is probably due to the proximity of meteorological stations, where precipitation has been measured in a consistent manner. Also, soil sampling was conducted by the same team, with a consistent, rigorous methodology over a short period of time. However, the strength of the correlation is surprising considering that dry deposition is not accounted for, although the high precipitation rate in much of Iceland means dry deposition is unlikely to contribute much to the total ^{137}Cs deposition. In addition, lateral transport by erosion would be expected in some Icelandic areas (Arnalds, 1999). A map of predicted ^{137}Cs deposition for Iceland, based on the AMAP methodology is given in Figure 3·52.

Overall, the AMAP methodology has been successful and has the advantage that it is possible to predict the ^{137}Cs deposition at any location in any year since 1960. Allthough fallout did occur prior to 1960, this was at lower levels than during the 1960s.

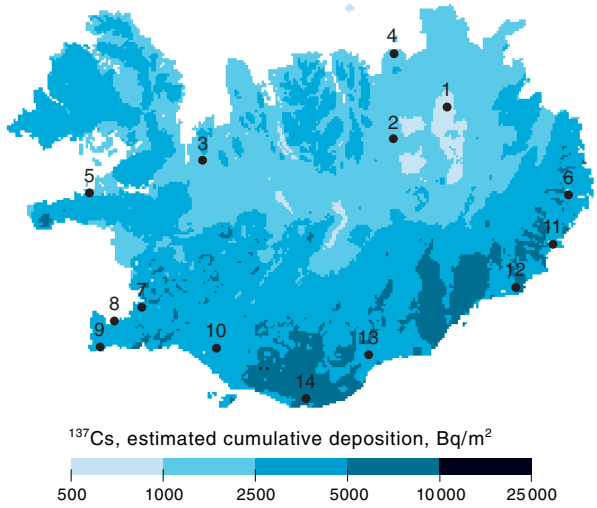

Figure 3·52. Preliminary map of estimated cumulative deposition of ^{137}Cs from atmospheric nuclear weapons tests, decay-corrected to 1995 (AMAP Data Centre). The map is based on a preliminary estimate of the average annual precipitation in Iceland, using a model developed by Crochet (2002) and precipitation data from 1960 to 1990. The conversion to deposition was achieved using a method equivalent to the AMAP method (Pálsson *et al.*, 2002a). Numbers indicate locations of sites represented in Figure 3·51.

3.7.3. Amchitka Island

In November 1971, the project Cannikin was conducted by the U.S. Atomic Energy Agency, now the Department of Energy, at the Amchitka Island underground nuclear test area; this was its largest underground nuclear test, with a yield of about 5 Mt. Preceding Project Cannikin were Projects Long Shot and Milrow; tests of approximately 80 kt and 1 Mt. These three tests represented an estimated 15 to 16% of the total effective yields of all the U.S. underground nuclear tests. In total effective yield, this site is the second largest and the only island underground nuclear test area in the United States. The location is shown in Figure 3·53.

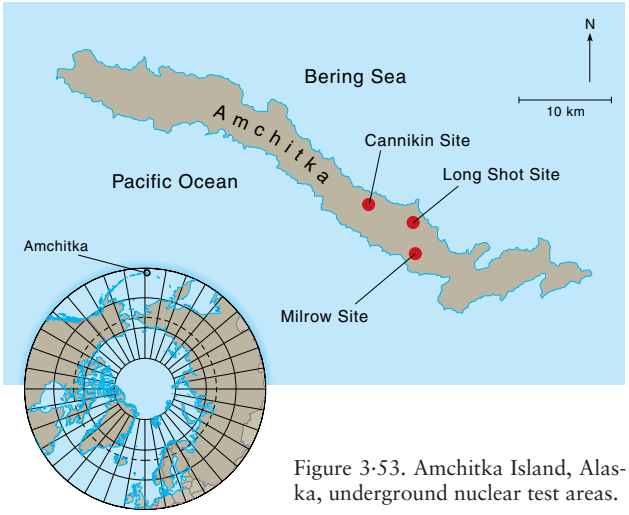

Figure 3·53. Amchitka Island, Alaska, underground nuclear test areas.

3.7.3.1. **Sampling**

Since the late-1970s there has been no marine sampling around Amchitka to assess the status of the anthropogenic radionuclides present or to determine trends. Groundwater contaminated by the three underground nuclear tests is transported toward discharge points on the ocean floor. Conceptual groundwater transport models have shown, based on a range of geohydrological assumptions, that discharge of radionuclides could have started as early as 1975; ten years after the first test.

In 1996, Greenpeace reported that leakage of ^{241}Am and $^{239+240}$Pu had been detected from these underground test sites to the terrestrial and freshwater environment (Miller and Buske, 1996). The marine environment was not specifically addressed in the Greenpeace report. In response, a federal, state, tribal, and non-governmental team conducted a terrestrial and freshwater radiological sampling program in 1997. Additional radiological sampling was conducted in 1998. An assessment of the reported leakage to the freshwater environment was evaluated by assessing tritium (^{3}H) values in surface waters and ^{240}Pu : ^{239}Pu ratios in various sample media (Dasher *et al.*, 2002). Tritium values ranged from 0.41 Bq/L ± 0.11 (2 SD) to 0.74 Bq/L ± 0.126 (2SD) at the surface water sites sampled, including the reported leakage sites. Only at the Long Shot test site, where leakage of radioactive gases to the near surface occurred in 1965, were higher ^{3}H levels of 5.8 Bq/L ± 0.19 (2SD) still observed in 1997; in mud pit #3 (Faller and Farmer, 1998). The mean ^{240}Pu : ^{239}Pu ratio for all Amchitka samples was 0.199 ± 0.014 (1 SD), with values ranging from 0.182 ± 0.0007 (1 SD) to 0.24 ± 0.02 (1 SD).

For the macroalga *Fucus distichus* the mean ^{240}Pu : ^{239}Pu atom ratio of 0.217 ± 0.016 (1 SD) is slightly outside the 95% confidence interval (±2 SD) of the reported global ratio of 0.176 ± 0.014 (1 SD) (Krey *et al.*, 1976). The mean ^{240}Pu : ^{239}Pu atom ratio of 0.216 ± 0.023 (1 SD) for the littoral zone marine sediment samples was consistent with the higher ratio seen for *F. distichus*. Deviations from the global fallout mean ^{240}Pu : ^{239}Pu atom ratio observed in marine algae, sediment, and pooled Amchitka samples may suggest another source of Pu to the marine environment. In an investigation of Bering Sea sediments Hameedi *et al.* (1999) reached similar conclusions. However, uncertainties in analyses and environmental processes must be fully assessed before making conclusions. Further work is needed to determine whether there are any other sources of Pu to the Bering Sea and North Pacific regions besides global fallout.

Results of the 1997 and 1998 sampling based on the measured ^{240}Pu : ^{239}Pu ratios and ^{3}H levels do not provide any evidence for leakage of ^{241}Am or other radionuclides from the underground test shot cavities into the terrestrial or freshwater environments on Amchitka Island (Dasher *et al.*, 2002). In addition, the hydrogeological regime as understood for Amchitka does not provide the physical means to transport transuranics from the test cavities to the reported surface locations.

Clearly, these results do not mean that leakage from the Amchitka underground nuclear tests is not occurring or will not occur into the North Pacific Ocean or the Bering Sea. Hydrogeological modelling predicts leakage can begin initially for ^{3}H from the test sites into the marine water over periods of 20 to 3000 years (Claassen, 1978; Dudley *et al.*, 1977). These periods bridge the various hydrogeological parameter assumptions that can be made. No sampling has been conducted in the marine environment surrounding Amchitka since the late-1970s and, thus, it remains an important area to be addressed.

3.7.3.2. **Geological forces**

Since the underground nuclear tests, dramatic changes have taken place in the field of geosciences and in the understanding of the geological forces acting on the Aleutian Islands, including Amchitka (Eichelberger *et al.*, 2002). In the 1960s, the site was considered geologically stable, showing little evidence of vertical tectonic motion or massive slope failures. Large ongoing horizontal displacements were not considered a possibility.

A paradigm shift occurred in the years following the nuclear tests with the acceptance of the theory of plate tectonics. Amchitka Island is now understood to be a fragment of an island arc crest at the intersection of the subduction of the Pacific Plate beneath the North American Plate (Figure 3·54). Recent field measurements (Eichelberger *et al.*, 2002) indicate that Amchitka is undergoing westward movement of about 1 cm/yr. This sug-

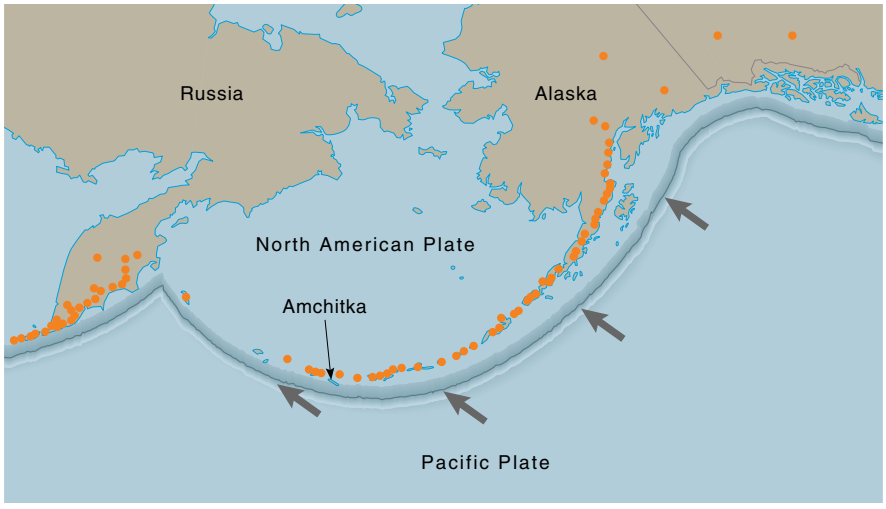

Figure 3·54. The Aleutain Vocanic Arc. Orange circles indicate active volcanoes. Arrows show the motion of the Pacific Plate relative to the North American Plate (Eichelberger *et al.*, 2002).

gests potential major faults in Amchitka Pass and also a strike-slip boundary north of Amchitka that is moving at a rate approximately two-thirds that of the San Andreas fault. The stresses induced would tend to open fractures perpendicular to the island leading into the marine environment.

The acceptance that Amchitka is part of a crustal block rotating clockwise within the fore-arc of an obliquely converging subduction zone raises concerns over possible enhancement of 'fast pathways' for the release of radionuclides from the underground nuclear test sites to the marine environment. Figure 3·55 provides a schematic illustration of the Cannikin underground nuclear test site over the adjacent Teal Creek Fault. A limited survey of the coastline near the Cannikin test area revealed a low density of joints, but did identify apparent fluid transport along these structures in the geological past. A better understanding of the geological forces affecting Amchitka is needed to determine their potential impact on leakage and in designing appropriate long-term monitoring programs.

3.7.3.3. Summary

The knowledge that environmental pathways, potentially enhanced by geological forces, exist on Amchitka Island to transport radionuclides into the nearshore marine environment is a cause for concern. The nearshore environment is commercially and environmentally important. An independently conducted radiological assessment is required to protect the indigenous peoples of the region (the Aleut), U.S. and Russian citizens, and people living off the vast commercial fisheries of the region (State of Alaska and Aleutian/Pribilof Island Association, 2001). The recent radiological assessment of the French nuclear test sites in the South Pacific provides an example of what is needed (IAEA, 1998b).

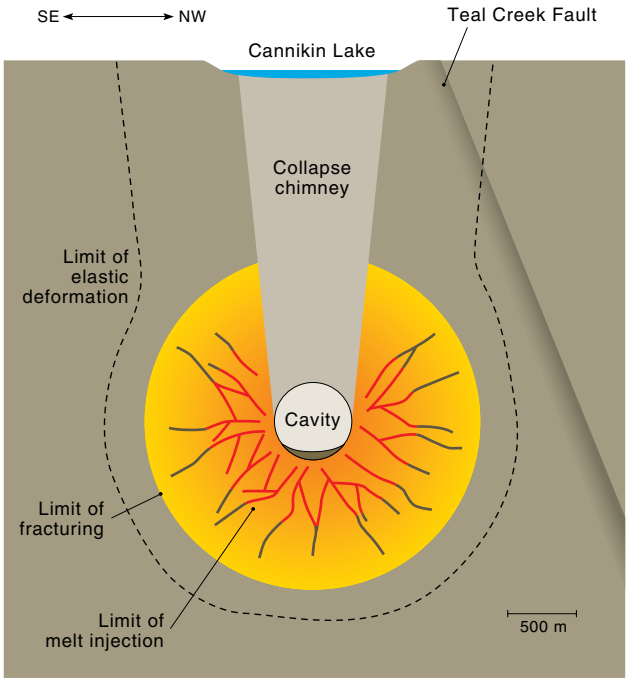

Figure 3·55. Schematic cross-section showing the effects of the Cannikin underground test, based on work by R. Laczniak and colleagues at the Nevada Test Site (Eichelberger *et al.*, 2002).

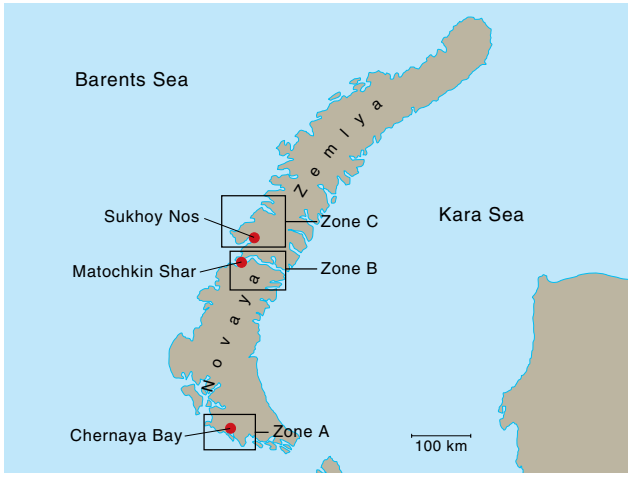

Figure 3·56. The central test site of the Russian Federation at Novaya Zemlya.

3.7.4. Novaya Zemlya

Since the first AMAP assessment, two further sources of information on Novaya Zemlya have been published: a report by Ivanov *et al.* (1997) and a major review of the Novaya Zemlya test site by Logachev (2000). The following information is based on these sources.

Novaya Zemlya was one of two major nuclear test areas for the former Soviet Union. Altogether, 130 nuclear tests had been carried out at the north test site by 25 October 1990 (the date the effective moratorium was announced). Nuclear tests were conducted in three areas (Figure 3·56):

Zone A. A series of nuclear tests were conducted from 1955 to 1962. The first underwater nuclear test occurred on 21 September 1955, the date of commencement for the site. The explosion comprised the experimental blasting of a T-5 torpedo with a warhead of about 3.5 kt at a depth of about 12 m. Another underwater test was conducted later. Six underground nuclear tests were conducted in vertical blast holes between 1972 and 1975, and there was a near-surface nuclear explosion on 7 September 1957.

Zone B. Thirty-three underground nuclear tests were conducted in tunnels within mountains between 1964 and 1990.

Zone C. A series of elevated and atmospheric nuclear tests, were undertaken commencing 24 September 1957 and ending 25 December 1962. The largest nuclear test explosion ever, a 58 Mt atmospheric blast, occurred in this zone on 30 October 1961.

3.7.4.1. Soil contamination

The data used by Ivanov *et al.* (1997) and Logachev (2000) are mainly from surveys by the E.K. Fedorov Institute of Applied Geophysics (in 1976 to 1978 and 1990) and the V.G. Khlopin Radium Institute (in 1992).

The ^{137}Cs contamination density outside the test areas ranged from 1.7 to 5.6 kBq/m^2 (45 to 150 mCi/km^2) in the 1976 to 1978 survey, with a mean of 3.4 kBq/m^2 (91 mCi/km^2). The contamination density in 1990 ranged from 1.5 to 6.7 kBq/m^2 (40 to 180 mCi/km^2) with a mean of 3.3 kBq/m^2 (90 mCi/km^2).

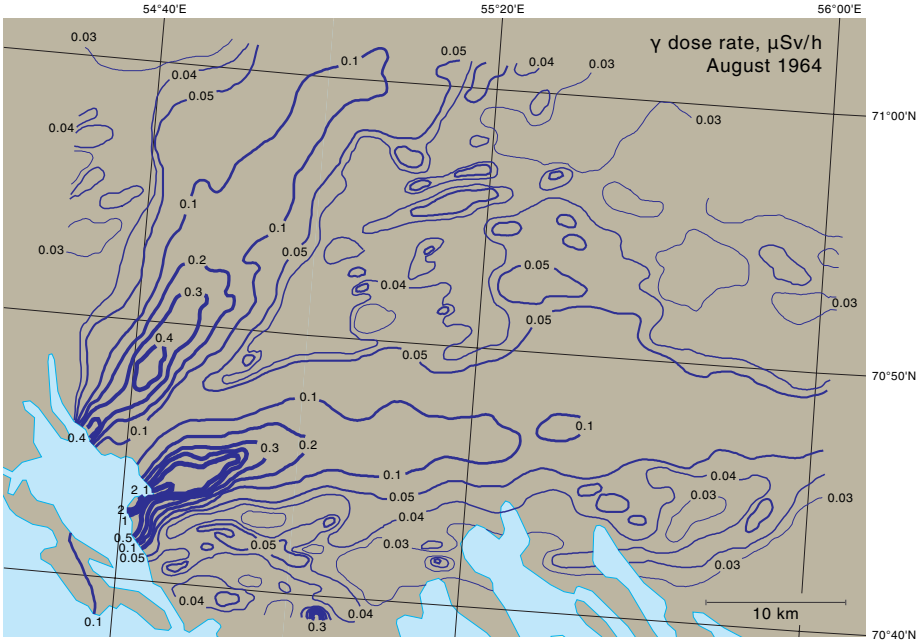

Figure 3·57. Radiation situation in the area around Chernaya Inlet in August 1964 (Ivanov *et al.*, 1997; Logachev, 2000). Contour lines show γ dose rates 1 m above ground.

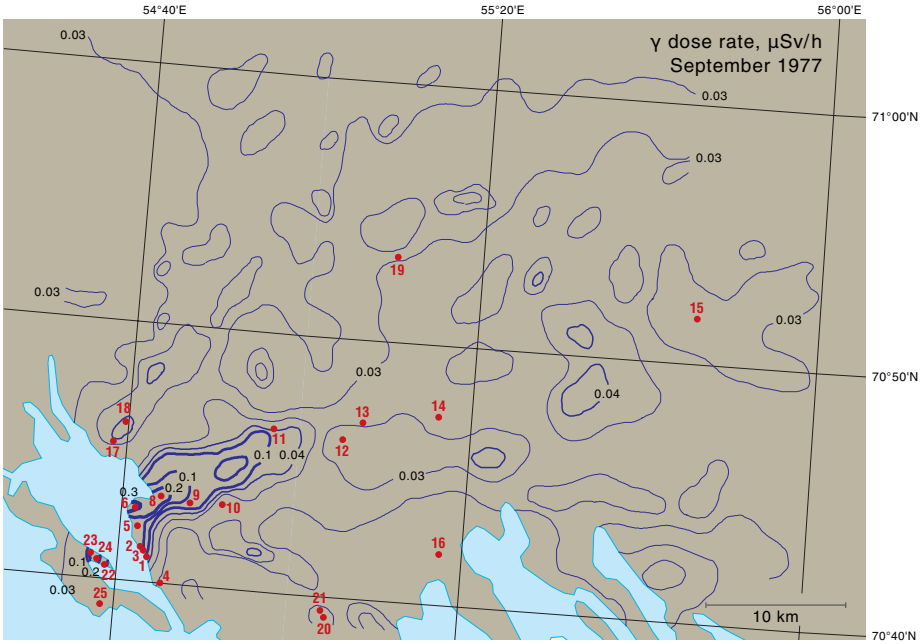

Figure 3·58. The radiation situation in the area of the Chernaya Inlet in September 1977 (Ivanov *et al.*, 1997). Contour lines show γ dose rates 1 m above ground. Red dots and associated numbers indicate sampling sites referred to in Table 3·19.

The surveys placed particular emphasis on studying radioactive traces due to deposition of radioactive products after the nuclear explosions. The zones of increased radioactive contamination detected during the survey include:

- the area around Chernaya Bay (Zone A);
- Sukhoy Nos Peninsula (Zone C);
- the area around Bashmachnaya Inlet (Zone B); and
- the tidal area of the Matochkin Shar Strait (Zone B).

The present assessment contains improved data for the first two sites; data for the others are available in the first AMAP assessment (AMAP, 1998).

3.7.4.2. **Area around Chernaya Bay**

Of the 90 atmospheric nuclear weapons tests conducted on the archipelago between 1955 and 1962 at least four were in contact with the underlying surface, and all occurred in the area of Chernaya Bay.

The epicenter of one of the explosions conducted in 1957 was about 100 m from the shore. The trace of the radioactive fallout from this explosion, as followed in the first three days after the explosion to a distance of 1500 km from the epicenter, covered part of the South Island and the Yamal, Gydansky, and Taymir Peninsulas. In 1964, another aerial survey was carried out over the extent of the trace covering 70 km along the axis and the results are shown in Figure 3·57. Analyses revealed the presence of the following radionuclides: ^{137}Cs, ^{144}Ce, ^{125}Sb, ^{106}Ru, ^{90}Sr, ^{60}Co, ^{152}Eu, ^{154}Eu, and ^{155}Eu. The epicenter of this near-surface explosion is the most contaminated zone on the archipelago. The measurements in this zone were repeated in 1976 to 1977. Results of the 1977 aerial survey and the location of soil sampling points are shown in Figure 3·58. The level of gamma radiation near the 1957 explosion funnel was as high as 5 μSv/h (the transverse size of the zone is several tens of meters). The distribution of the radionuclides was investigated using depth samples collected from two

Table 3·18. Radionuclide profiles for soils (Bq/kg (10^{-9} Ci/kg)) collected in 1977 from the epicenter of the near-surface nuclear explosion conducted in 1957 in the area of Chernaya Inlet, Novaya Zemlya (Ivanov *et al.*, 1997; Logachev, 2000).

Depth, cm	^{137}Cs	^{60}Co	^{152}Eu
Site 1			
0-1	67000 (1800)	52000 (1400)	Trace
1-2	70000 (1900)	44000 (1200)	Trace
2-3	44000 (1200)	33000 (900)	17000 (460)
3-4	19000 (520)	22000 (590)	18000 (480)
4-5	12000 (320)	22000 (590)	22000 (590)
10-15	2300 (61)	27000 (720)	54000 (1450)
20-25	–	8700 (235)	17000 (460)
30-35	70 (1.9)	13000 (360)	2500 (67)
40-45	330 (8.9)	190 (5.1)	440 (12)
50-55	230 (6.1)	–	–
60-65	160 (4.2)	–	–
Site 2			
0-2	41000 (1100)	32000 (870)	4400 (120)
2-4	46000 (1250)	26000 (710)	6700 (180)
4-6	50000 (1350)	26000 (715)	7000 (190)
6-8	27000 (725)	16000 (425)	8000 (215)
8-10	23000 (610)	12000 (325)	7800 (210)
10-15	16000 (430)	13000 (360)	6800 (185)
20-25	13000 (360)	4100 (110)	8500 (230)
30-35	190 (5)	–	1900 (50)
40-45	110 (3)	120 (3.3)	250 (6.8)
50-55	–	–	–
60-65	46000 (3.8)	–	–

pits; located 10 m southwest of the funnel crest (site 1, Figure 3·58) and 100 m north of the funnel (site 2, Figure 3·58). Data on the local distribution of γ-emitters for these samples are shown in Table 3·18.

The extent of the radioactive trace is decreasing with time. The area of the trace exceeding 0.1 μSv/h decreased from 133 km^2 in 1964 to 10 km^2 in 1977 (see Figures 3·58 and 3·59). Moreover, the trace has become heterogeneous in character, due to radioactive decay of short-lived γ-emitters.

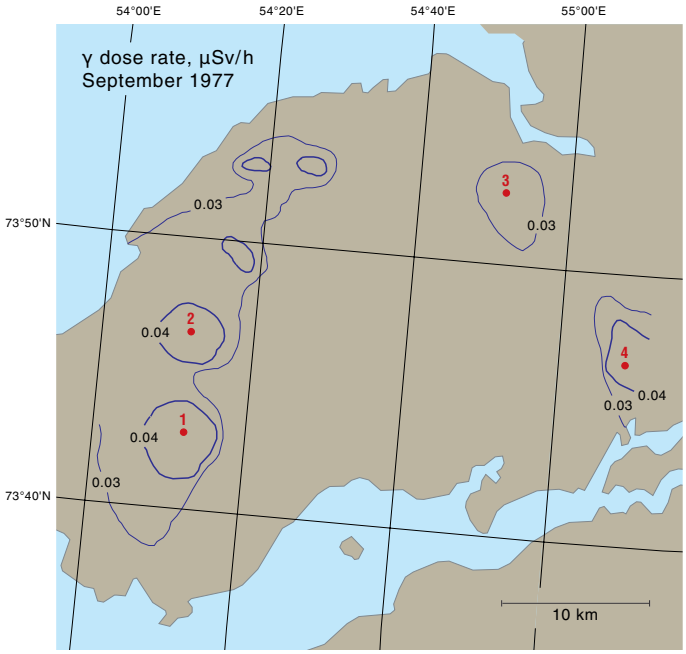

Figure 3·59. The radiation situation on the Sukhoy Nos Peninsula in September 1977. The radiation dose rate was in excess of natural background (Logachev, 2000). Red dots and associated numbers indicate contaminated sites referred to in the text.

In addition to the trace resulting from the near-surface explosion of 1957, traces of radioactive contamination from an above-water explosion in 1961 and an underwater explosion in 1955 can be seen in Chernaya Bay. Data on the density of contamination by radionuclides in these traces obtained in 1977 are shown in Table 3·19.

3.7.4.3. Sukhoy Nos Peninsula

Most of the atmospheric nuclear weapons tests were conducted above the Sukhoy Nos Peninsula to the north of the Matochkin Shar strait. Several areas of contamination resulted from these tests. A gamma survey and soil sampling campaign carried out in 1977 showed four contaminated areas (see Figure 3·59):

- the western trace is an area (0.5 km^2) 3 km east of the Fedorov Mountain (Site 1);
- the central trace (0.3 km^2) is in the center of the peninsula (Site 2);
- the northern trace (0.3 km^2) is 10 km from the Tsivolki Cape (Site 3); and
- the eastern trace (0.4 km^2) is 12 km northeast of the Klochkovsky Peninsula (Site 4).

Table 3·20 shows the man-made radionuclides in soil from the eastern trace. These data suggest that contamination after the elevated air explosions, during which mineral (soil) particles were generally not entrained in the plume, was primarily due to radionuclides formed as a result of interaction between the neutron flux of the penetrating radiation arising from the nuclear explosion and the soil.

3.7.5. Thule

In January 1968, a B-52 aircraft carrying four nuclear weapons crashed onto the sea ice ~11 km from Thule Air Base in northwest Greenland (see Section 2.4). As a consequence, the benthic marine environment of Bylot Sound (180 to 230 m deep) became contaminated by ^{239,240}Pu. The site was revisited in August 1997, 29 years after the accident. Sections 3.7.5.1. to 3.7.5.4. are extracted from Dahlgaard *et al.* (2001).

3.7.5.1. Plutonium in water and seaweed

Activity concentrations of ^{239,240}Pu in *Fucus distichus* (a brown alga) around Thule and 750 km to the south near Uummannaq ranged from 0.15 to 1.14 Bq/kg dw. The source of most of this Pu is global fallout – except possibly the highest value seen in a single sample near the accident site. With the exception of a near-bottom water sample taken at the point of impact containing 30 mBq/m^3, no clear effect of the accident was seen in any of the water samples. Of this elevated level, 42% was particulate indicating that resuspended sediments containing accident-related Pu are an important source. The general level of ^{239,240}Pu within Bylot Sound was 5 to 10 mBq/m^3 in unfiltered surface water, which is regarded as global fallout background. These data indicate that Pu from contaminated sediments is not transported into surface waters in significant quantities.

Table 3·19. Radionuclide profiles for soils (kBq/m^2 (mCi/km^2)) collected in 1977 from within the traces of nuclear explosions in the Chernaya Bay area (Ivanov *et al.*, 1997).

	No. of site in Fig 3·58	Sample No.	Depth, cm	^{137}Cs	^{90}Sr	^{60}Co	^{152}Eu
Epicenter zone	1		0-5	4800 (1.3×10^5)	–	2800 (7.5×10^4)	780 (2.1×10^4)
and near-surface	2		0-5	4100 (1.1×10^5)	–	2400 (6.4×10^4)	280 (7600)
explosion trace	3		0-3	26 (690)	–	160 (4200)	230 (6300)
1957			3-6	20 (540)	–	160 (4200)	190 (5200)
			6-10	7.8 (210)	–	130 (3500)	200 (5400)
	4		0-5	14 (380)	–	–	–
	5		0-5	85 (2300)	–	59 (1600)	–
	6	1	0-5	160 (4400)	100 (2700)	190 (5200)	–
		2	0-2	21 (560)	–	24 (650)	5.4 (140)
			2-4	5.2 (140)	–	4.8 (130)	0
			4-6	–	–	–	–
		3	0-2	37 (1000)	–	78 (2100)	8.1 (220)
			2-4	–	–	–	–
	7		0-5	74 (2000)	–	89 (2400)	–
	8		0-5	11 (310)	4.8 (130)	10 (280)	–
	9		0-5	7.8 (210)	–	5.9 (160)	–
	10		0-5	30 (800)	–	24 (660)	–
	11		0-5	2.6 (69)	–	–	–
	12		0-2	11 (310)	–	10 (270)	–
			2-4	3.5 (94)	–	3.3 (88)	0
			4-6	–	–	–	0
	13		0-5	5.7 (155)	0.93 (25)	2.7 (72)	–
	14		0-5	9.3 (250)	–	5.2 (140)	–
	15		0-5	3.9 (106)	3.7 (100)	–	–
	16		0-5	2.6 (69)	–	–	–
Trace of above-	17		0-5	48 (1300)	70 (1900)	–	–
water explosion	18		0-5	5.2 (140)	–	–	–
1961	19		0-5	2.3 (61)	–	–	–
Spot resulting from	20	1	0-5	–	–	120 (3300)	220 (5900)
near-surface			10-15	–	–	56 (1500)	110 (2900)
explosion			20-25	–	–	12 (330)	23 (630)
			30-35	–	–	–	–
		2	0-1	0.96 (26)	–	4.4 (120)	7.4 (200)
			1-2	–	–	13 (350)	23 (610)
			2-3	–	–	28 (770)	46 (1250)
			3-5	–	–	63 (1700)	96 (2600)
	21		0-5	2.6 (69)	2.9 (79)	–	4.4 (120)
Trace of the	22*		0-3	300 (8000)	–	48 (1300)	–
the underwater			3-6	160 (4400)	–	34 (930)	–
explosion 1955			6-10	44 (1200)	–	10 (270)	–
	23		0-2	410 (11000)	–	56 (1500)	–
			2-4	160 (4300)	–	29 (780)	–
			4-6	26 (700)	–	7 (190)	–
			6-8	41 (1100)	–	9.8 (265)	–
			8-10	59 (1600)	–	–	–
	24		0-5	44 (1200)	3.7 (100)	8.5 (230)	–

* no vegetation on the sampling location.

Table 3·20. Radionuclides in soil (kBq/m^2 (mCi/km^2)) from the eastern part of the experimental zone (Site 4) on the Sukhoy Nos Peninsula in early-1993 (Ivanov *et al.*, 1997; Logachev, 2000).

Sample No.	Depth, cm	^{137}Cs	^{60}Co	^{152}Eu
#1	0-1	1.4 (37)	Trace	2.7 (72)
	1-2	1.4 (37)	Trace	3.7 (100)
	2-3	0.85 (23)	Trace	4.4 (120)
	3-4	Trace	Trace	5.6 (150)
	4-5	Trace	Trace	5.9 (160)
#2	0-5	2.6 (70)	19 (520)	36 (980)
	10-15	Trace	Trace	23 (610)
	20-25	Trace	Trace	Trace
	30-35	Trace	Trace	Trace
#3	0-5	2.2 (60)	15 (400)	14 (380)
#4	0-5	3.5 (95)	Trace	20 (550)
#5	0-5	4.6 (125)	12 (330)	31 (830)

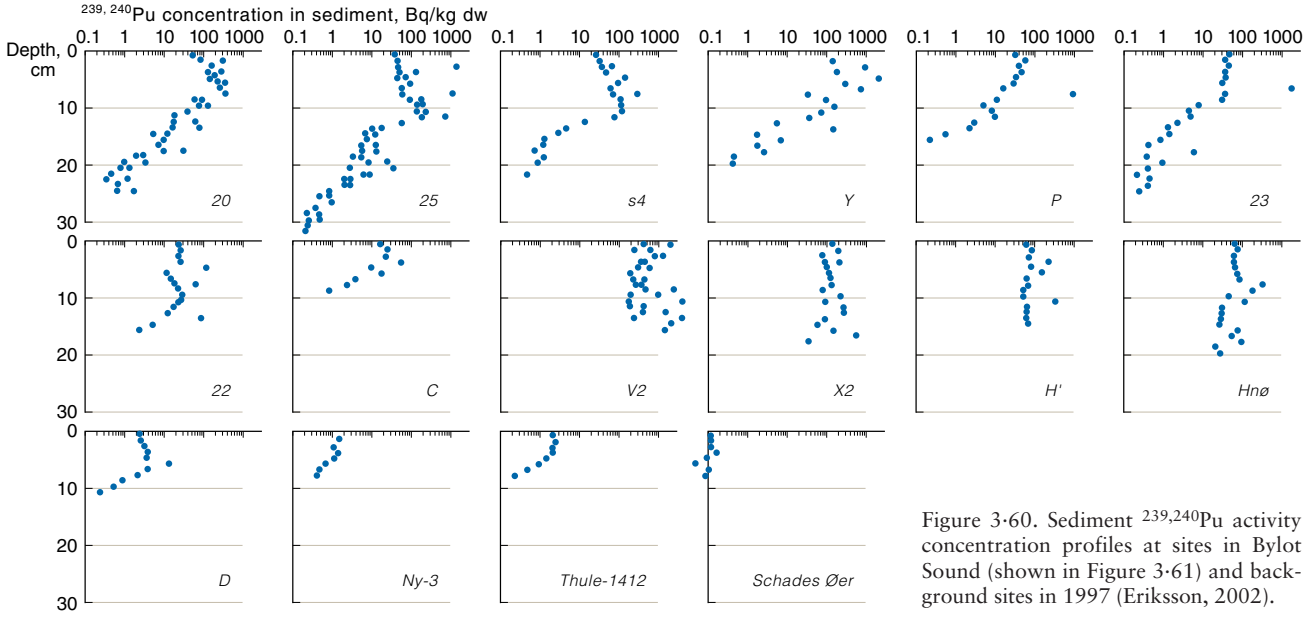

Figure 3·60. Sediment ^{239,240}Pu activity concentration profiles at sites in Bylot Sound (shown in Figure 3·61) and background sites in 1997 (Eriksson, 2002).

3.7.5.2. **Sediments**

Figure 3·60 shows Pu depth profiles for contaminated sediment cores from Bylot Sound, plus background cores taken outside Bylot Sound (Ny-3, Thule-1412, and Schades Øer; the latter about 750 km southeast of Thule). In all cases, the Pu appears well mixed throughout the upper 3 to 5 cm layer (note the logarithmic concentration axis in Figure 3·60). Despite logarithmic axes, the large variation in Pu concentrations is clear. This is caused by 'hot particles'. In a recent thesis Eriksson (2002) stated that these 'hot particles' hold more Pu than previously anticipated (see Section 2.4).

Plutonium concentrations in surface (0 to 3 cm) sediments are shown in Figure 3·61. The highest concentrations are centered on the accident site, with a fairly even distribution in the remaining deep part of Bylot Sound, and almost fallout background concentrations outside Bylot Sound. The water depths at the accident site – close to location V2 – are 180 to 230 m. The two assumed background sites outside Bylot Sound, Ny-3 and Thule-1412, have depths of 500 and 640 m. A surface (0 to 3 cm) ^{239,240}Pu activity concentration of 0.12 Bq/kg dw occurred 750 km further south near Schades Øer. Surface concentrations outside Bylot Sound (at Thule-1412 and Ny-3) are an order of magnitude higher. It is unclear whether this reflects accident Pu or a natural perturbation caused by differences in sedimentological parameters. At other Arctic marine locations similar levels of Pu have been attributed to global fallout (see Section 3.3.4).

3.7.5.3. **Benthic biota**

Plutonium concentrations in biota have been compared with concentrations in surface (0 to 3 cm) sediments (Figure 3·61) to give 'concentration ratios' (Table 3·21). Although the biota live within or on the sediments the concentration ratios indicate that the bioavailability of the weapons Pu is low. Most of the concentration ratios fall within the range 0.01 to 0.1, i.e., Pu concentrations in benthic biota are around one to two orders of magnitude lower than in surface sediments. Furthermore, a significant proportion is probably not metabolized but is bound to particles within the gut and adheres to the surface structure of the animals. One single bivalve sample had a much higher level, which was probably due to a 'hot particle'.

3.7.5.4. **Isotope ratios**

A number of the sediment samples were analyzed for ^{240}Pu : ^{239}Pu atom ratios by High Resolution Inductively Coupled Plasma/Mass Spectrometry. These had ratios in the range 0.027 to 0.057. The calculated uncertainties for most of the samples were 2 to 10%. The samples with highest activity – which have been identified as containing 'hot particles' – show significant variation in the ^{240}Pu : ^{239}Pu atom ratios, i.e., there is a variation in Pu isotope ratios in the Thule debris significantly above measurement error. This supports the conclusion by Mitchell *et al.* (1997) that the Thule Pu originates from at least two sources of different quality. Plutonium concentrations in the samples for this study were dominated by the Thule weapons accident. Therefore, the higher

Table 3·21. Plutonium (^{239,240}Pu) concentration ratios (based on values in Bq/kg dw) for benthic biota and surface (0 to 3 cm) sediments (Dahlgaard *et al.*, 2001).

		Mean	SD	n
Mollusks	Bivalves	0.025	0.024	13
	Macoma calcarea	37*		1
	Snails	0.0033	0.0018	9
	Squid, *Rossia* sp.	0.00036		1
Echinoderms	Starfish	0.0094	0.0139	9
	Brittle stars	0.013	0.016	4
	Feather stars	0.0070	0.0060	4
	Sea urchins	0.12	0.16	4
	Sea cucumber	0.0080	0.0083	4
Crustaceans	Shrimp	0.0048	0.0088	4
	Various	0.038	0.039	4
Annelids	*Pectinaria* sp.	0.068	0.052	4
	Various	0.023	0.033	10
	Tube	0.28	0.29	6
Fish	*Liparis* sp.	0.00035		1

* outlier, probably caused by 'hot particle'.

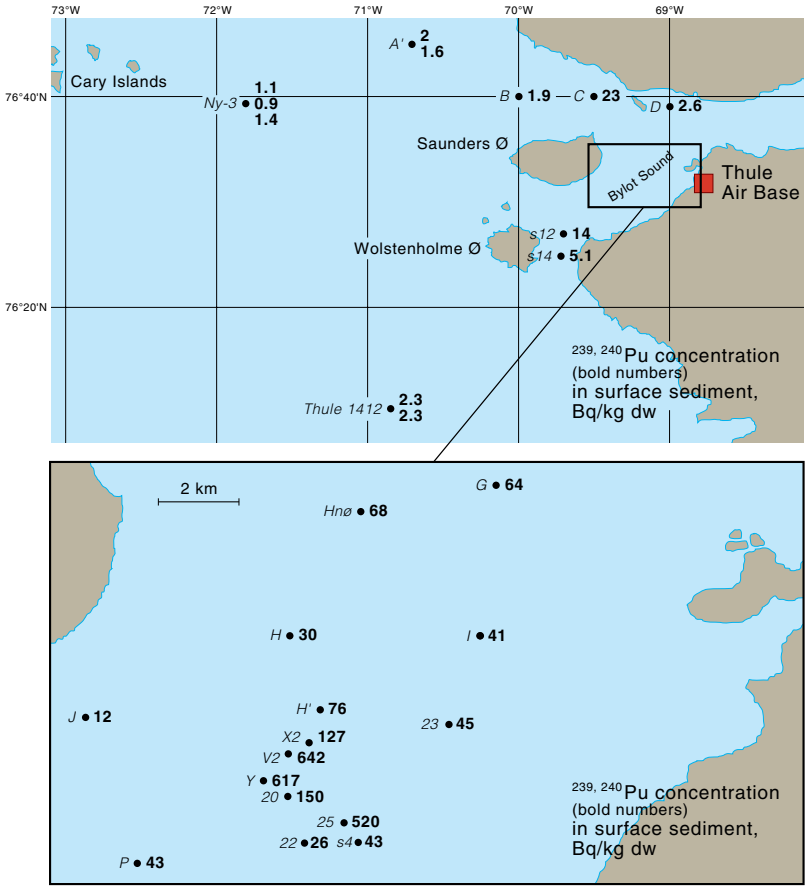

Figure 3·61. Activity concentrations of ^{239,240}Pu in surface sediments (0 to 3 cm layer) near Thule in 1997. Location names are shown in italics, concentrations in bold. The point of impact was on the sea ice (180 m water depth) at the location marked V2 (Eriksson, 2002).

^{240}Pu : ^{239}Pu atom ratio observed in global fallout, approximately 0.18, will not affect these results. Any influence of the higher ^{240}Pu : ^{239}Pu atom ratios in Sellafield discharges, up to around 0.25, is even more unlikely as the Sellafield-derived Pu concentration in the Thule area is accepted to be less than global fallout.

Average isotope ratios for ^{240}Pu : ^{239}Pu atom ratios, and ^{238}Pu : ^{239,240}Pu and ^{241}Am : ^{239,240}Pu activity ratios for sediment samples containing >20 Bq ^{239,240}Pu/kg, i.e., at least an order of magnitude above the fallout background, are given in Table 3·22. The reference date is the sampling date, 1997. By comparing the ^{241}Am : ^{239,240}Pu activity ratios for sediments (Table 3·22) with those for benthic biota (Table 3·23), it is evident that some biota appear to have a higher uptake of americium (Am) than Pu. This appears to be the case for mollusks – bivalves as well as snails – and for some echinoderms, namely brittle stars (Ophiuroidea) and starfish (Asteroidea), but not sea urchins (Echinoidea) or sea cucumber (Holothurioidea). This greater affinity for Am than Pu is not new. The International Atomic Energy Authority reported higher concentration ratios for Am than Pu in mollusks (IAEA, 1985).

Table 3·22. Isotope ratios in Thule sediment samples with >20 Bq ^{239,240}Pu/kg in August 1997 (Dahlgaard *et al.*, 2001).

		Mean	SD, %	n
^{240}Pu : ^{239}Pu	atom ratio	0.045	15	30
^{238}Pu : ^{239,240}Pu	activity ratio	0.014	53	223
^{241}Am : ^{239,240}Pu	activity ratio	0.13	61	114

Table 3·23. ^{241}Am : ^{239,240}Pu activity ratios in sediment-dwelling benthic biota, Thule 1997 (Dahlgaard *et al.*, 2001).

		Mean	SD, %	n
Benthos	All	0.39	76	84
Mollusks	All	0.63	62	24
Polychaetes	All	0.28	77	16
Crustaceans	All	0.22	36	5
Echinoderms	Brittle stars	0.55	24	4
	Starfish	0.41	34	11
	Sea urchins	0.17	8	5
	Sea cucumber	0.13	67	2

3.8. Summary

Since the first AMAP assessment, monitoring of various man-made radionuclides in the Arctic environment has continued to a variable degree. In general, concentrations of radionuclides derived from global fallout, from the Chernobyl accident, and from earlier discharges from European reprocessing plants are slowly decreasing, as expected. This is especially evident for ^{90}Sr, where global fallout is still the dominant source. It is also the case for ^{137}Cs, although the contribution from the Chernobyl accident and reprocessing discharges during the 1970s and 1980s has added significantly to the fallout level and still constitutes a source to the Arctic marine environment owing to remobilization and relocation processes. More unexpectedly, evidence is mounting that the Pu being remobilized from Irish Sea sediments is now responsible for a major proportion of the Pu contamination in the Norwegian and Barents Seas.

Data for the Faroe Islands and Iceland were not adequately dealt with in the first AMAP assessment.They have therefore been addressed in significantly greater detail in the present assessment.